Aalto University
School of Chemical
Engineering

**Tekendra Timsina**

# TEMPERATURE PROFILE CONTROL OF A MULTIPLE HEARTH FURNACE FOR KAOLIN CALCINATION

Master´s Programme in Chemical, Biochemical and Materials Engineering
Major in Chemical and Process Engineering

Master's thesis for the degree of Master of Science in Technology
submitted for inspection, Espoo, 30 March 2017.

| | |
|---|---|
| Supervisor | Professor Sirkka-Liisa Jämsä-Jounela |
| Instructor | Ph.D. Alexey Zakharov |
| | Ph.D. Jukka Kortela |

Aalto University
School of Chemical
Engineering

Aalto University, P.O. BOX 11000, 00076 AALTO
www.aalto.fi

**Abstract of master's thesis**

| | |
|---|---|
| **Author** | Tekendra Timsina |
| **Title of thesis** | Temperature profile control of a multiple hearth furnace for kaolin calcination |
| **Department** | Chemical and Metallurgical Engineering |
| **Major** | Chemical and Process Engineering |
| **Thesis supervisor** | Professor Sirkka-Liisa Jämsä-Jounela |
| **Thesis advisor(s) / Thesis examiner(s)** | Ph.D. Alexey Zakharov / Ph.D. Jukka Kortela |
| **Date** 30.03.2017 | **Number of pages** 63 **Language** English |

**Abstract**

The main aim of this thesis is to develop a new temperature profile control strategy for kaolin calcination in the multiple hearth furnace (MHF) in order to improve the quality of the product. The overall control strategy for the MHF is developed as a three level control hierarchy: optimizing level, stabilizing level, and basic level.

In the literature part of the thesis, first, the kaolin and its formation process is discussed. Next, the general information about calcination process is provided and the calcination of kaolin is discussed. Finally, few past researches having similar objective to this study are reviewed to study the various different control approaches developed so far and the possibility to implement them in our study.

In the experimental part, analysis of the process is carried using the experimental data. During the data analysis, activation/ deactivation of the exothermic reaction in the hearth 4 is seen, which is crucial in determining the temperature profile of the furnace. Hence, the soft sensor based on the energy balance to estimate the intensity of the exothermic reaction, which plays a key role in developing the control strategy for the MHF, is developed.

Both the static and dynamic energy balance equations are presented, calculated and compared in order to study the dynamic behaviour in the process. It is seen that the dynamic energy balance provides more accurate results than the static energy balance due to the consideration of the transition period.

**Keywords** Temperature profile, control, multiple hearth furnace, calcination, exothermic, kaolin

## Preface

This master's thesis is a part of STOICISM (The Sustainable Technologies for Calcined Industrial Minerals) project of the Research Group of Process Control and Automation, at Aalto University School of Chemical Technology. STOICISM is a major innovative research project supported by the European Commission under the 7th Framework Programme, for the "New environmentally friendly approaches to mineral processing". The thesis work lasted a period of six months, from 01. April 2016 to 30. September 2016.

Above all, I would like to thank my supervisor Professor Sirkka-Liisa Jämsä-Jounela for providing me an opportunity to complete my thesis work in this project. The encouragement and guidance she has provided me to complete my thesis work were supportive and welcoming. Further, I would like to thank my main advisor Dr. Alexey Zakharov for the great support and guidance throughout this period. Second advisor Dr. Jukka Kortela lent his assistance throughout the project and I am thankful for his supports.

I wish to acknowledge all the co-workers (Ibrahim, Jose, Azadeh, Rinat, Nelli, Susanna, Babak, and Kai) for their helpful suggestions and friendly working environment. Along with the co-workers, I would also like to thank all my friends and relatives who have directly and indirectly helped me during my study.

I would also like to express my gratitude to my family in Nepal for their support and encouragement. Last but not the least; I want to thank my beloved wife Anjula Ghale Timsina for her endless love and support during my study.

Espoo, 30.03.2017

Tekendra Timsina

## Abbreviations

| | |
|---|---|
| B | Burner |
| BZT | Burning Zone Temperature |
| EGH | Encapsulated Graphite Heaters |
| ERR | Exothermic reaction rate |
| FBF | Fluidized Bed Furnace |
| FFC | Feedforward Control |
| FOPDT | First Order plus Dead Time |
| H | Hearth |
| HVAC | Heating, Ventilation, and Air-Conditioning |
| ID | Induced Fan |
| MHF | Multiple Hearth Furnace |
| MPC | Model Predictive Control |
| OTF | Optical Fiber Thermometers |
| PI | Proportional-Integral |
| PID | Proportional-Integral-Derivative |
| PRBS | Pseudorandom Binary Sequences |
| SISO | Single Input Single Output |
| T | Temperature |

## Notations

| | |
|---|---|
| $C_{p,k}$ | Heat capacity of kaolin [J/(g*K))] |
| $C_{p,mk}$ | Heat capacity of kaolin [J/(g*K))] |
| $C_{p,w}$ | Heat capacity of water [J/(g*K))] |
| $F_4$ | Gas flow in the hearth 4 [$m^3$/s] |
| $F_6$ | Gas flow in the hearth 6 [$m^3$/s] |
| H(i) | Hearth number, where i = 1 to 8 |
| $H_{comb}$ | Heat of combustion of methane [J/mol] |
| $Q_{comb}$ | Energy produced by combustion of methane [J/s] |
| $Q_{h(i)}$ | Energy consumed in hearth (i) [J] |
| $\dot{Q}_{dehyd}$ | Energy consumed by the dehydroxylation reaction [J/s] |
| $\dot{Q}_{evap}$ | Energy of water evaporated from the solid [J/s] |
| $\dot{Q}_{g,in}$ | Enthalpy of inflowing gas [J/mole] |
| $\dot{Q}_{g,out}$ | Enthalpy of outflowing gas [J/mole] |
| $Q_{sg}$ , $Q_{gs}$ | Energy transfer between the solid and the gas phase [J/s] |
| $\dot{Q}_{s,in}$ | Enthalpy of incoming solid [J/mole] |
| $\dot{Q}_{s,out}$ | Enthalpy of outgoing solid [J/mole] |
| $\dot{Q}_{spin}$ | Energy released by the spinel phase formation reaction [J/s] |
| r | Exothermic reaction intensity indicator [%] |
| $T_i$ | Temperature in the hearth i [℃] |
| $V_{meth}$ | Flow of methane to the burner [$m^3$/s] |

# Table of Contents

# 1. Introduction

Minerals are the naturally occurring substance found in abundant scale and possess some economic value. Minerals can be used in their raw stage or can be processed to high-value materials. Kaolin, also known as china clay, is a white industrial mineral generally used in a wide range of industries, such as paint, paper coating, rubber and plastic as a functional filler. It is also used as a raw material for ceramics and fiber glass products. Kaolin consists of kaolinite ($Al_2Si_2O_5(OH)_5$ as a principal mineral.

Calcination is a thermal treatment process where the kaolin is processed at high temperature to remove water and to obtain the calcined kaolin with higher properties and economic value. The calcined kaolin possesses more whitish and chemically inert properties, which broadens its application area. During calcination, the kaolin undergoes a series of physicochemical reactions at different temperatures. The reaction process begins with removal of free moisture at around 100-150 °C, followed by the dehydroxylation reaction at around 400-600 °C, where the amorphous metakaolin is formed by the removal of chemically bounded water. The third reaction occurs at around 980 °C where the metakaolin is transformed to the spinel phase by re-crystallization. The hard mullite is formed at the temperature above 1050 °C (Eskelinen, 2014).

Multiple hearth furnace (MHF), a common technology used for the calcination of kaolin, is considered during this study. The MHF used, in this study, consists of 8 hearths with counter current solid and gas flow. Similarly, the energy for calcination is provided through the fuel burners in hearths 4 and 6. The quality of the calcined kaolin is dependent on the temperature profile over the furnace and needs to be controlled in order to obtain desired quality products. Currently, the temperature in hearths 4 and 6 is controlled through adjustment of the fuel gas (methane gas) flow. This gas flow determines the amount of combustion air. (Eskelinen, et al., 2015)

The temperature measured in the hearths is also correlated with the temperature of the solid beds and the gas flowing from adjacent hearths. The past studies reveal that process variables of hearths 4 and 5 are interrelated and thus, controlling the temperature in hearth 4 shows the significant effects in the hearth 5. A similar result was found in hearths 6 and 8. However,

the controlling of temperature only in hearths 4 and 6 results in variations of the temperature profile in the furnace, and therefore, temperature control in the whole furnace should be considered to improve the product quality control. The aim of this thesis is to develop a method to control the temperature profile of the multiple hearth furnace.

This thesis work is mainly divided into two parts: the literature part and the experimental part. The chapters are organized as follows. Chapter 2 provides the general background information about kaolin and its formation. Chapter 3 describes the process. Chapter 4 introduces few past research studies having the objective to maintain a stable temperature profile in the furnace. Chapter 5 ,6, 7, and 8 discusses about the experimental task done. Chapter 9 presents the conclusion.

# 2. Processing of Kaolin

Kaolin, also known as china clay, is a soft white or nearly white industrial minerals primarily used as a coating in the paper industry. It also has application as a functional filler in rubber and plastic industries, as raw materials in ceramics, in fiber glass products and others. Kaolinite ($Al_2Si_2O_5(OH)_5$ is the principal mineral component in the kaolin comprising 10-95% in the commercial grade kaolin along with other many impurities (Pruett & Pickering, 2006). The presence of common impurities, such as iron oxides, hydroxides, smectites, silica, feldspar, mica, and quartz reduces the value of kaolin.

The kaolin is found in the form of rock in nature and is of little use in its natural stage. The kaolin goes through the extensive process called kaolinization before it can be used as a product. Kaolinization is an extensive process where the kaolin is formed by the decomposition of aluminum silicate mineral or other clay minerals (The Great Soviet Encyclopedia, 1970-1979).

## 2.1 Formation of kaolin

The mining of kaolin clays is generally carried out in open pits and the mined clays are refined to enhance the quality of kaolin. The refined grade kaolin is dried to remove the moisture. The kaolin is now ready to use or can be thermally processed for special application such as cosmetic and medical applications. The kaolin formation and processing are briefly described below. (Thurlow, 2005; Pruett & Pickering, 2006)

### 2.1.1 Pit Operations

The kaolin pit operations begin in an open area with the removal of overburden (a layer of top soil). After the overburden has been removed, the un-uniform granite, also called hard ground, is broken down by drilling the whole (up to 15m) and blasting it with the use of explosive emulsions. The quality of the clay is inspected by observing the small piles of fine sand and dust produced during drilling.

The kaolinised granite obtained after blasting is further processed to obtain clay. The processing can be done by two different ways. In a traditional method called “washing the

clay face", a jet of water is directed to the site to break down the kaolinised granite into rocks, stones, sands, and clay. The rocks and stones settled down at the bottom, which are then separated from sands and clay. Currently, the modern method called "dry mining method" has been adopted by large pits where the kaolinised graphite is extracted by the excavator and deposited to the fixed site called "make down plants". The kaolinised granite deposited in the make down plants by excavator is then washed by water jets to break down and release clay, sand, and stones from the kaolinised granite. The suspension of clay, sand and mica released during wash flows to the lowest point in the pit and needs to be extracted. The extraction to the higher level is done by using centrifugal pumps which are then delivered to the sand removal plant. The removal of sand can be done by an old method called settling pits, where sand is allowed to settle from clay in a large pits or troughs. However, slow and laborious settling pits method has been currently replaced by modern and efficient bucket wheel classifiers methods (conveyor methods), where the fine particles, clay, and mica are separated from coarse particles due to their different settling time.

The separated particles still contain fine sand and coarse mica, which need to be removed. The removal of fine sand and coarse mica from the clay occurs in the circular, tapered pipe called hydroclone. The wash containing clay, fine sand, and coarse mica is pumped to the hydroclone, where the coarse mica is separated from fine clay and mica by the centrifugal forces. The particle size is separated into two grades: over 50 microns (coarse) and less (fine). The separated fine clay and mica (smaller than 50 microns) suspension is sent for the refining process.

### 2.1.2 Refining Process

The suspension extracted from pits operations also contains fine sand and mica along with fine clay and thus need to be separated to obtain pure fine clay. Initially, the clay is thickened before refining. The suspension is pumped into the large circular tank where the thickening is carried out. The settled clay is removed from the bottom central outlet of the tank by the slow moving raking arms. The flocculent is added in the tank to enhance the settling of clay as they cluster together and settle down faster. The collected clay is then pumped to one refinery where various properties such as color, particle size, and viscosity are tested before they are sent for the refining.

The refining of thickened clay begins with the removal of fine mica. The removal of fine mica can be done either using a hydroclassifier (raked tanks) or a hydroclone (closed vessel). The hydroclones are the special equipment used for sorting of suspension. In the hydroclassifiers, the clay in the suspension is deflocculated by the addition of the alkaline chemical. Due to the effect of de-flocculent, the clay particle remains suspended for some time, whereas the coarser fine mica settles down to the bottom of the tank and is removed by the pump. Alternatively, fine mica is removed from the thickened clay in hydroclones in a similar manner as described in hydroclassifiers. The thickened clay is fed to a hydroclone of a larger internal diameter (125 mm) and the clay overflow from it is re-treated in a hydroclone of a smaller internal diameter (50 mm). The underflow collected is grinded for a short period of time considering the unwanted underflows collected might contain curled stack of fine clay possessing similar size to fine mica. The clay in a curled stack is easy to break and hence the grinding should be done for a short time ensuring no any fine mica grinding occurs. The ground material is then treated in hydroclones for the overflow of clay.

Hydroclassifier/Hydroclone refined china clay might still contain some iron-containing impurities, such as mica, iron oxides, and tourmaline and thus need to be separated. The presence of such impurities can cause specks in ceramic ware when fired and as a result, reduces the brightness of clay used for paper coating. Hence, magnetic separation process (use of powerful electromagnet) is used for the removal of the impurities containing iron. This separation process can be carried out using two different kinds of machines both capable of using a super-conducting electromagnet to create high magnet field with the low electric current. The machine used to separate coarse clays is a large electromagnet with a circular chamber in a center. The chamber is filled with stainless steel wool and the iron-containing impurities attach in that magnetized steel wool. The magnetic particles attached are flushed in each electromagnetic cycle by switching of the magnet and introducing the clear water. A machine used for fine clays contains a pair of reciprocating canisters packed with wire wool moving in and out of a super-conducting magnetic field. The slight magnetic particles of the clay are controlled on the wire wool matrix of canisters. The canisters work in ensuring the continuous process.

The final refining process to form pure clay is bleaching. The staining of clay by iron oxides is common and hence the bleaching is done to recover the brightness of the clay by converting the insoluble iron oxides into soluble iron sulphate with the use of sodium hydrosulphite solution. Due to its soluble properties and being less colored, iron sulphate is

lost during the drying stage. The bleaching of clay is carried out in two steps; first, the clay is passed through the tall tower where air trapped in the clay is removed, and then, the clay passes through the pipe system where sodium hydrosulphite is added.

### 2.1.3 Drying

Refined china clay is transported to a drying plant via pipeline. The refined clay might contain some clay in a deflocculated state and thus thickening of clay is carried out to flocculate it. The flocculation is carried out with the addition of acid where the clay settles down quickly and the clear water is removed from the top of the storage tank leaving the thickened clay.

The thickened clay goes through the filter pressing stage to reduce the water content of clay. The thickened clay is pumped under increased pressure to the filter presses, a series of rectangular or circular chambers lined with a tightly woven nylon cloth, which allows water to pass though it capturing the clay cake. The clay cake formed by filter pressing has about 25-30% water content. Filter pressing can also be done in tube presses at a higher pressure as an alternative to commonly used circular or rectangular presses. The clay cake is passed through the cylindrical pug mill to increase the flow properties of clay particles by making it round. This process is important for paper coating industries where a smooth flow of clay onto the continuous sheet of paper is required at higher speed. The clay particles are then pelletized down to about a centimeter (cm) for a better drying. Initially, the clay is mixed and the lumps formed are broken down in an enclosed trough with paddles. The mixed clay is then conveyed to a pelletizing drum enclosing a rotating, vertical shaft with pegs. The desirable clay pellets for convenient drying is formed by this pelletizing process.

Now, the clay is ready to be dried. The drying can be done in two different kinds of the dryer; a Buell tray dryer and a Fluidized bed dryer. A Buell tray dryer consists of a stack of trays (about 30 layers) arranged in a circular tower attached to central rotating columns. The rotation of the rotating columns is done by a current of hot air supplied into the dryer by a fan. The clay to be dried is fed into the top trays of the rotating tower and it is eventually pushed down to the following trays and subsequently conveyed to the bottom of the dryer in about forty-five (45) minutes by the fixed arms. The moisture content of the dried clay is about 10%. Fluidized bed dryer is a modern method for drying china clay. It is a horizontal

cylindrical chamber where the hot air with slight pressure for drying of clay is supplied through the perforated floor. The pressurized hot air fluidizes the pellets of clay fed into the chamber, resulting in the quicker and uniform drying of pellets. The vibrational movement of the perforated floor in an elliptical motion due to the special arrangement of the drying cylinder further enhances the drying of clay. Fluidized bed dryers are categorized into two types based on the presence/absence of the cooling unit within the dryer. The fluidized bed dryer containing both drying and cooling units helps to reduce dust levels outside, minimizes the steam emissions from the dried product, and it is more suitable for lower tonnages with drying capacity of about 3000 tons per week whereas a dryer with a separate drying and cooling unit has drying capacity of around 6000 tons per week.

The refined and dried kaolin (china clay), which is obtained as pellets can now be sold to various industries for different applications. However, the clay can be further processed according to the customer demands. Since, paint, rubber, and plastics use the clay in powder form, it is also milled into dry powder or even delivered as a slurry, especially to the paper industry. Also, the kaolin can be calcined (thermal treatment) for the special quality products. The calcination of kaolin will be discussed further in section 3.

# 3. Calcination

The kaolin undergoes a process called calcination for the improvement of its properties. Calcination is the thermal treatment of an ore in the presence of oxygen to decompose and eliminate the volatile products as well as any impurities present in an ore and thus produces value-added products (Ghosh & Ray, 2001; Murray, 2006). The calcination process is carried out in a large furnace called a calciner at a higher temperature, up to 1500 ℃. Calcination was initially developed for the metal industries to burn metal to its oxide form, however, it is now a common thermal treatment process in mineral industries. Calcination of limestone sludge, limestone, kaolin clay, and cement clinker are few typical examples in mineral industries whereas the process was also adopted for waste combustion and energy production. (Mcketta & Cunningham, 1978;Smith, 2005)

A rotary kiln is the commonly used calciner, however, various other calciners are used in practice, such as a multiple hearth furnace, a calciner, and a fluidized bed calciner. A calciner is generally divided into two zones; burning zone and cooling zone. The burning zone is further categorized into various sub-zones (pre-heating zone, calcination zone) based on the temperature. This thesis study focuses on calcination of kaolin in a multiple hearth furnace. The ore to be calcined is fed to the burning zone where the thermal treatment process is carried out for a specific time-period at the desired temperature profile, which is then passed through the cooling zone to cool down before they are collected from the discharge end (Mcketta & Cunningham, 1978).

The calcination method is categorized in two different ways based upon their calcination time: flash calcination and soaked calcination. A flash calcination method is a rapid thermal treatment process where the flash calcination process is performed in a relatively short time (from few seconds to few minutes), contrary to the soak calcination where the complete calcination takes longer time (about an hour). The soak calcination method has been considered as an efficient method due to complete hydroxylation contrary to flash calcination, where only partial dehydroxylation takes place due to the short time (Salvador, 1995). In addition, it was found that properties of soak calcined products differ from flash calcined products. However, the industries have been recently adopting the flash calcination method considering its economic aspect due to a short residence time. Also, the development

of technology capable of controlling the degree of dehydroxylation over a wide range of temperature has enhanced the demand of flash calcination (Rasmussen, et al., 2015).

## 3.1 Kaolin calcination

The fine kaolin obtained after the refining and drying process may contain some impurities, such as feldspar, mica, and quartz. Some impurities in the kaolin are removed during calcination and the obtained kaolin after calcination is termed as calcined kaolin. Calcination of kaolin not only removes the impurities but also enhanced the various properties of kaolin such as hydrophobicity, brightness, abrasive nature, optical properties, and electrical properties and thus adds the value of the kaolin (Chandrasekhar , et al., 2002). Kaolin loses its absorbed water at about 100 ℃, whereas it goes through the various phase transformation on further heating. The kaolin undergoes the endothermic dehydroxylation reaction and metakaolin formation starts at about 450 ℃ and continues until the temperature reaches around 800 ℃. Metakaolin is commonly used as a pigment in paper coating, a raw material for porcelain etc. The dehydrated amorphous metakaolin transformed into crystalline aluminosilicate spinel phase along with some free amorphous silica when heated to exothermic reaction temperature (around 950 ℃) (Insley & Ewell, 1935). On further heating kaolin to the temperature above 1050 ℃, mullite is formed along with silica. Mullite is a needle-shaped crystalline aluminosilicate used for the manufacturing of refractory material. The amorphous silica changes into a crystalline structure called cristobalite on heating above 1200 ℃. Heating rate during calcination, size, and shape of kaolin to be processed, the presence of impurities, and residence time distribution are the important properties to consider during calcination as they have the significant effect in the properties of calcined kaolin (Thomas, 2010). The kaolin undergoes the phase transformation reactions (Ptáček, et al., 2010).

$$\underset{(Kaolinite)}{Al_2O_3.2SiO_2.2H_2O} \xrightarrow{\sim 500\ ℃} \underset{(Metakaolininte)}{Al_2O_3.2SiO_2 + 2H_2O} \quad (1)$$

$$\underset{(MetaKaolinite)}{2(Al_2O_3.2SiO_2)} \xrightarrow{\sim 950\ ℃} \underset{(Al-Si\ Spinel)\ (Amorphous)}{3Si_3Al_4O_{12} + SiO_2} \quad (2)$$

$$\underset{(Al-Si\ Spinel)}{Si_3Al_4O_{12}} \xrightarrow{>1050\ ℃} \underset{(Mullite)}{2(3Al_2O_3.2SiO_2)} + \underset{(Amorphous)}{5SiO_2} \quad (3)$$

$$\underset{(Amorphous)}{SiO_2} \xrightarrow{\geq 1200\ ℃} \underset{(Cristoballite)}{SiO_2} \quad (4)$$

# 4. Temperature profile control along the calciner

The kaolin is thermally treated to enhance its properties, such as hydrophobicity, brightness, abrasive nature, optical properties, and electrical properties. Since, the quality of the calcined product heavily depends on the temperature profile along the furnace/ kiln/ oven, the stable desired temperature is crucial for production of optimal quality products (Zhou, et al., 2004; Stadler , et al., 2011; Valiquette, et al., 1997; Akalp, et al., 1994). Also, as discussed earlier the end product obtained from the calcination varies upon the temperature. Thus, the study on temperature profile along the furnace is of major interest for efficient control strategy development. However, controlling the temperature in the industrial processing calciner is very challenging due to various factors. Temperature control in the process is very complex as a furnace is considered as a multi-zone system having multiple inputs and outputs with non-linear, and time-varying behavior. Also, the cross-coupling effect between the variables representing different zones (hearths) increases the difficulties in maintaining the temperature profile (Galvez & de Araujo, 1996; Zhou, et al., 2004; Moon & Lee, 2000). Thus, the desired temperature profile frequently cannot be obtained by controlling the temperature independently by implementing conventional control methods. There are numerous researches performed to find effective control methods to maintain the desired temperature profile.

This chapter introduces few research studies having the objective to maintain a stable temperature profile in the furnace. The literature review represents some important research studies that aimed to find the optimal control methods for desired and stable temperature profile. The literature on temperature profile control on the kilns is also considered along with the work related to the MHF, considering that calcination and control principles resemble each other in both cases.

## 4.1 Decouplers for better temperature profile

As mentioned earlier, in a multivariable process, the undesired cross-coupling occurs when the input variable of a control loop affects the output variable of another control loop. The cross-coupling effect causes the variation in the controlled variables resulting in the poor temperature profile. The cross-coupling effects between the control loops are compensated with the introduction of the decouplers. A decoupler is an additional transfer function block

added to the single-loop controllers, which aims to compensate for the disturbance in a control loop caused by operations of another loop. The single-loop controllers and the decouplers form the multivariable decoupling controller, in which the control loop are independent to each other due to compensation on the cross-coupling effect. The decouplers have been implemented in few research studies performed to control the variation in temperature, due to cross coupling between the zones (Ogunnaike & Ray, 1994).

Galvez & de Araujo (1996) designed a controller for a large industrial electrical tubular oven. In order to control the temperature profile of the oven carefully, the oven was divided into six heating zones and six controlled temperatures. However, there was a strong cross-coupling effect seen between the zones due to the heat flow, and which results in continuous variations in the temperature of each zone. Thus, controlling of the multi-zone system is complicated due to this cross-coupling effect between the adjacent zones and hence the multivariable frequency domain techniques was applied by Galvez & de Araujo (1996) to overcome this serious difficulty in maintaining the temperature profile of the oven.

The control process of the system is non-linear due to the different time constant for heating and cooling as well as due to unidirectional and saturation characteristics of the power source. However, under some specific operating condition, the system performed linearly allowing a linear analysis and design. A linear model was obtained and validated by performing several dynamic tests. Considering the cross-coupling effect of neighboring zones, the following tri-diagonal 6 * 6 matrix transfer function model was built.

$$G(s) = \begin{bmatrix} G_{11(s)} & G_{12(s)} & 0 & 0 & 0 & 0 \\ G_{21(s)} & G_{22(s)} & G_{23(s)} & 0 & 0 & 0 \\ 0 & G_{32(s)} & G_{33(s)} & G_{34(s)} & 0 & 0 \\ 0 & 0 & G_{43(s)} & G_{44(s)} & G_{45(s)} & 0 \\ 0 & 0 & 0 & G_{54(s)} & G_{55(s)} & G_{56(s)} \\ 0 & 0 & 0 & 0 & G_{65(s)} & G_{66(s)} \end{bmatrix} \quad (5)$$

where, $G_{ii(s)} = \frac{10.8\, e^{-t}}{68.7s+1}$, $G_{ij(s)} = \frac{5.25\, e^{-25t}}{108.33s+1}$

$$Y(s) = [y_{1(s)} \;\; y_{2(s)} \;\; y_{3(s)} \;\; y_{4(s)} \;\; y_{5(s)} \;\; y_{6(s)}]^T \quad (6)$$

$$U(s) = [u_{1(s)} \;\; u_{2(s)} \;\; u_{3(s)} \;\; u_{4(s)} \;\; u_{5(s)} \;\; u_{6(s)}]^T \quad (7)$$

The researchers figure out that obtaining the steady state temperature profile is their most critical objective. Hence, low-frequency decoupling at 0 rad/s in the closed-loop system was obtained by implementing an inverse gain matrix as a decoupling pre-compensator to ensure a satisfactory steady-state temperature profile control. The following decoupling pre-compensator matrix, which behaved as a diagonal dominant matrix at low frequencies, was obtained.

$$K_1 = G(0)^{-1} =$$

$$\begin{bmatrix} +0.1467 & -0.1113 & +0.0822 & -0.0579 & +0.0368 & -0.0179 \\ -0.1113 & +0.2289 & -0.01692 & +0.1191 & -0.0758 & +0.0368 \\ +0.0822 & -0.1692 & +0.2658 & -0.1871 & +0.1191 & +0.0822 \\ +0.0822 & +0.1191 & -0.1871 & +0.2658 & -0.01692 & +0.0822 \\ +0.0368 & -0.0758 & +0.1191 & -0.01692 & +0.2289 & -0.1113 \\ -0.0179 & +0.0368 & -0.0579 & +0.0822 & -0.1113 & +0.1467 \end{bmatrix} \quad (8)$$

Where, $u^* = [0.0787 \quad 0.0286 \quad 0.0529 \quad 0.0529 \quad 0.0286 \quad 0.0787]^T$

A PI controller designed for this model is as follows.

$$K_2 = K_p \left(1 + \frac{1}{T_i s}\right) I \quad (9)$$

where $Kp = 3$, $T_i = 80$

Hence, the multivariable controller was built by combining the pre-compensator and the PI controller, which was given as,

$$K(s) = K_1 K_2(s) \quad (10)$$

The closed loop transfer function matrix of the system was finally given by,

$$G(s) = [I + G(s)K(s)]^{-1} G(s)K(s) \quad (11)$$

The block diagram of the system is shown in Figure 1.

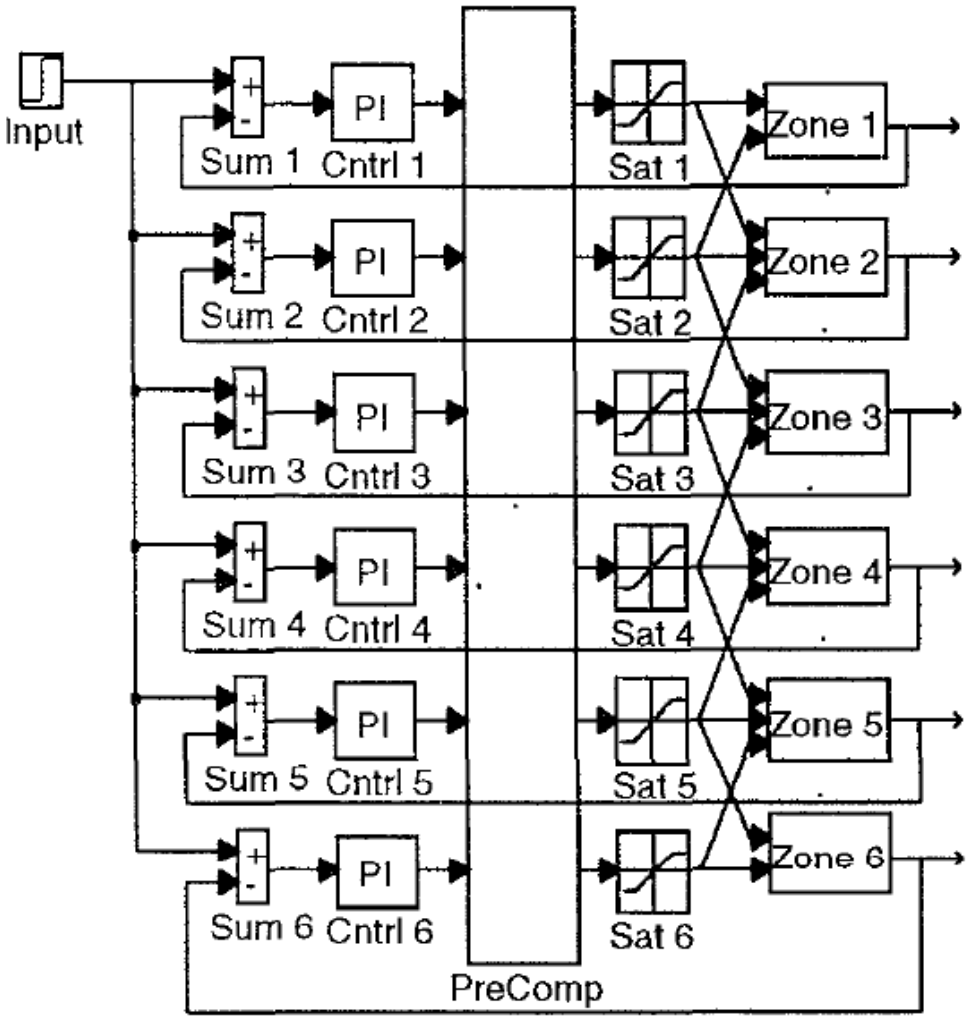


Figure 1: Block diagram of the system (Galvez & de Araujo, 1996)

Carrying out simulation experiments, the multivariable controller was validated. The partial bode diagrams were obtained for the open loop system with and without a decoupling pre-compensator. The high level of interactions observed between the zones was found to be compensated by the implementation of the decouplers. Negligible cross-coupling gains were observed at low frequencies for the system with a decoupling pre-compensator. Figures 2 and 3 obtained from the experiments showed the comparison between open loop step responses of a zone in the absence/presence of the compensator.

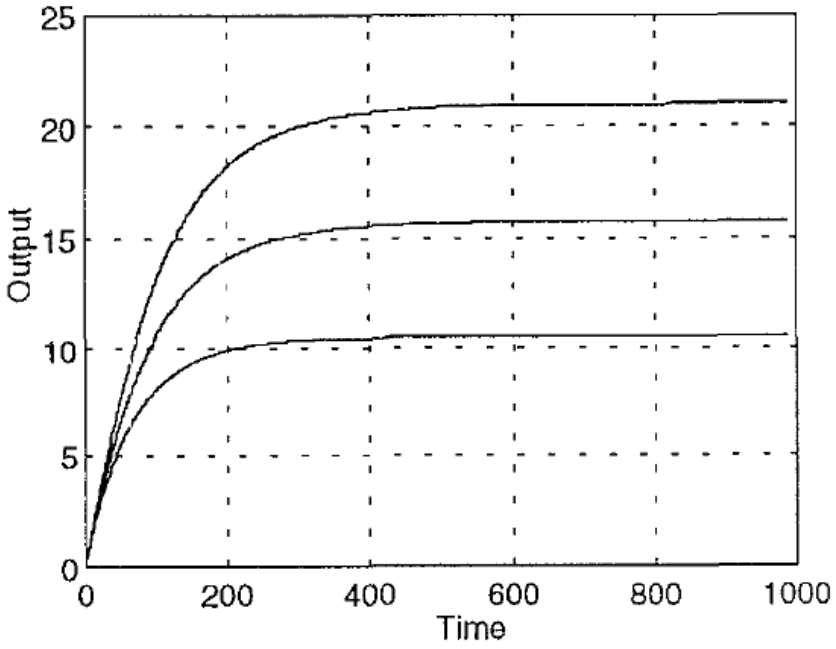


Figure 2: Open loop response of a zone without compensator (Galvez & de Araujo, 1996)

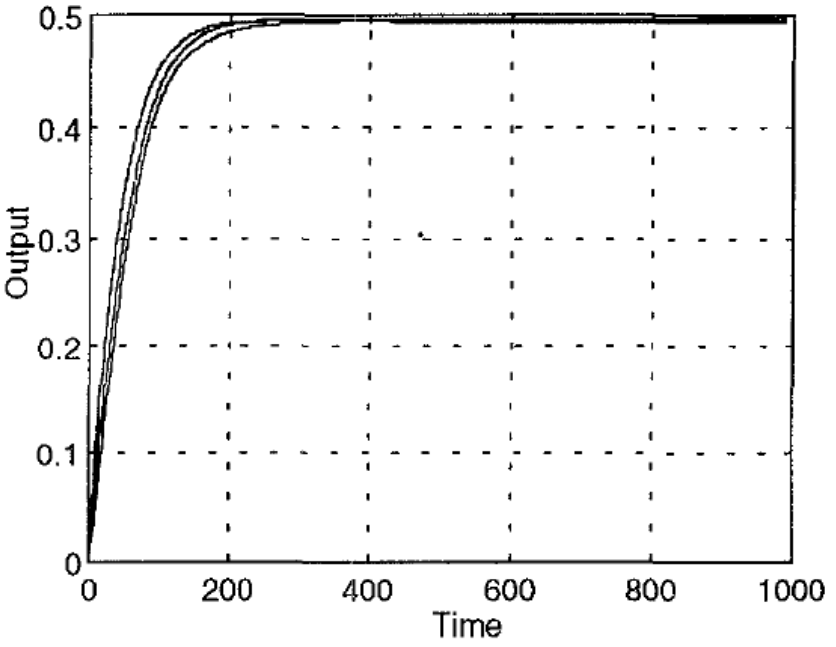


Figure 3:Pre-compensated open loop response of a system (Galvez & de Araujo, 1996)

Similar to the previous research, Zhou, et al. (2004) describes the temperature measurement and control system of a large (31m) vertical quench furnace using decouplers. The radial temperature distribution of the furnace used for thermal treatment of aluminum alloy for

forging was studied to ensure the desire quality product. The vertical quench furnace was divided into eleven zones and each zone was equipped with a heating element and thermocouple. The schematic diagram of a furnace is represented in Figure 4 below.

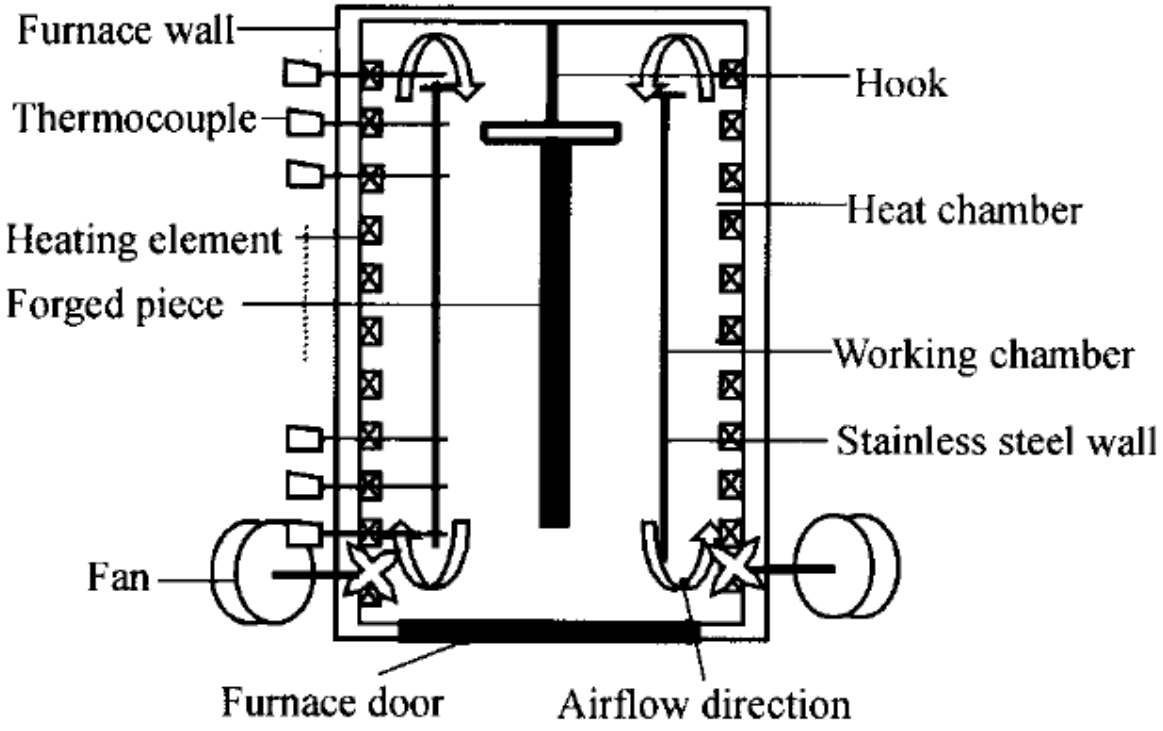


Figure 4: Simplified diagram of a quench furnace *(Zhou, et al., 2004)*

The forged piece was vertically held in the furnace and it was heated rapidly to the desired temperature. When the desired temperature was achieved in the furnace, it was held at that temperature for the specific time period to obtain the sample of desired quality. Hence, the temperature in the furnace is divided into two sections; rising period and holding period. As in the previous case, the system was found to be very complex due to various characteristics of the system, for example non-linear, time-varying, multiple inputs/multiple outputs. Additionally, due to the strong coupling between the zones, it was discovered that the temperature of a zone was affected by the temperature of adjacent zones. The study further added that accurate model formulation of the furnace as well as precise control of the temperature distribution in the furnace by a closed loop PID and predictive algorithm were not achieved due to the complexity of these tasks. Along with the above-mentioned difficulties, it was also noticed that the temperatures measured by the thermocouple were

actually the furnace air temperatures not the temperature of the solid forged piece and hence, the desired temperature on the solid was nearly unattainable.

Hence, this study was focused on achieving the desired temperature of the solid by studying the radial temperature measurement and adjusting it by implementing the multivariable decoupling self-learning PID control algorithm. The thermodynamic equilibrium equations were formulated to study the radial temperature distribution of the system. The calculation then yields the difference between the temperature of the forged piece and the actual measurement. The calculated difference was then used as a compensator in the actual measurement during holding period, which eventually gives the temperature of the forged piece.

The closed coupling multivariable system was decoupled to eleven (11) independent subsystems and each subsystem was controlled by a self-learning PID algorithm. The decoupling between the adjacent zones was only considered due to the fact that non-adjacent zones were only considered to have a little effect that could be neglected. The following Figure 5 demonstrates the block diagram of an $i^{th}$ simplified branch, followed by its algorithm in Equation 12.

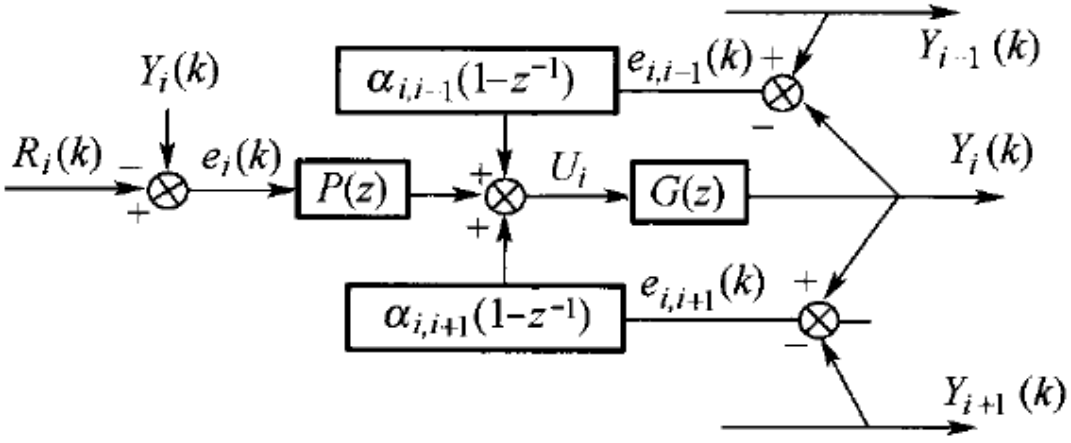


Figure 5: Block diagram of the simplified branch *(Zhou, et al., 2004)*

$$\Delta u_i(k) = K_{p,i}\{e_i(k) - e_i(k-1)\} + \frac{T_0}{T_{I,i}} e_i(k) + \frac{T_{D,i}}{T_0}\{e_i(k) - 2e_i(k-1) + e_i(k-2)\} + \alpha_{i,i-1}(k)\{e_{i,i-1}(k) - e_{i,i-1}(k-1)\} + \alpha_{i,i+1}(k)\{e_{i,i+1}(k) - e_{i,i+1}(k-1)\} \quad (12)$$

where $K_{p,i}$ , $T_{I,i}$ , $T_{D,i}$ are the proportional, integral, and differential factors of PID controller in the i[th] zone, $T_0$ is the control period, $e_i(k)$ is the temperature error of the zone whereas $e_{i,i-1}(k)$ and $e_{i,i+1}(k)$ are the temperature differences between the neighboring zones. As it can be seen form Equation (12), $\alpha_{i,i-1}e_{i,i-1}$ and $\alpha_{i,i+1}e_{i,i+1}$ are the decoupling terms taking into account the effect of the adjacent zones, where $\alpha_{1,0}(k) = \alpha_{11,10}(k) = 0$.

From above equations, it is noted that the coupling effect depends on the temperature difference between the zones. The values of the decoupling coefficient, $\alpha_{i,i-1}$ and $\alpha_{i,i+1}$ were considered to be zero (0) during the rising period due to the fact that the temperature correlation was not critical at this stage. During the holding period, the initial values of the decoupling coefficient were automatically obtained by using the specific rules developed based on the temperature difference. Accordingly, the parameters $K_{p,i}$ , $T_{I,i}$ , $T_{D,i}$ were tuned online by the self-learning incremental PID control algorithm.

Figure 6 explains the control process of the i[th] branch. For the simplicity, the whole process was divided into three stages. The rising period was further divided into two stages, which categorizes the whole process into three stages. The proportional control algorithm was adopted in the initial stage. The initial proportional gain value ($K_{p,i}$) was increased/ decreased upon the parameter increment value ($\Delta K_{p,i}$) which was obtained from the comparison between the rising time in that stage and the set of the upper bounds on that stage. Similarly, the PID control algorithm was adopted in the second stage which leads to the determination of $K_{p,i}$ , $T_{I,i}$ , and $T_{D,i}$ values based upon the overshoot and the rising time. PI control algorithm was adopted in the final stage where $K_{p,i}$ and $T_{I,i}$ were changed to the values obtained by the PI tuning using the experimental data.

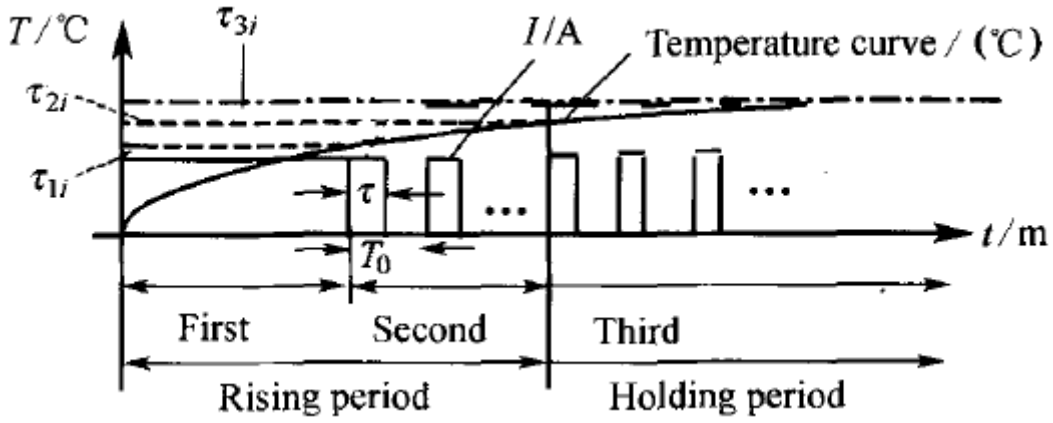


Figure 6: Graphical representation of the control process of a branch *(Zhou, et al., 2004)*

Figure 7 reveals that coupling effect between the zones was successfully compensated by the multivariable decoupling self-learning PID control algorithm as the uniformity in temperature was seen within 2% between the zones (chambers).

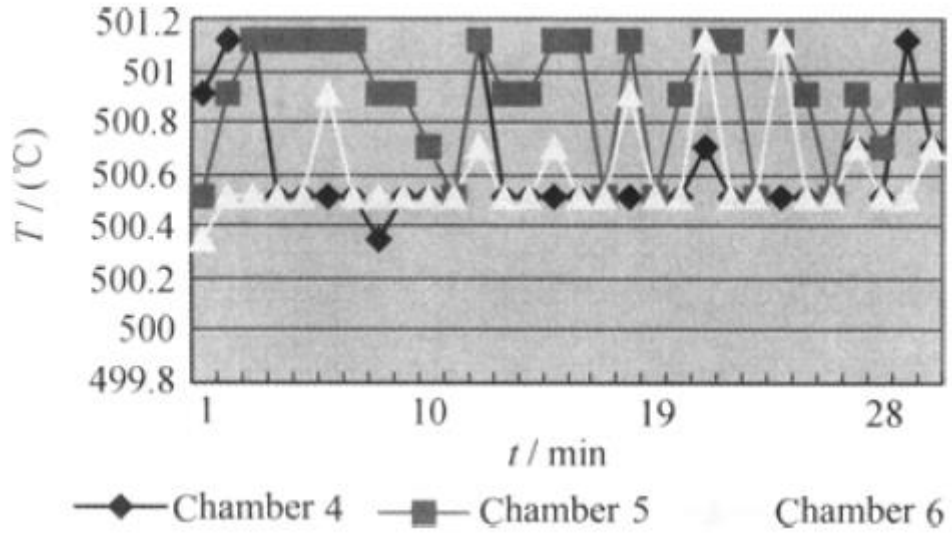


Figure 7: Temperature curves in the holding period (Zhou, et al., 2004)

Sauermann, et al.(2001) described similar decoupling methods to maintain the desired and stable temperature profile in multizone furnaces. The research study was carried out in four (4) zone furnace where strong thermal coupling was noticed between the zones. Hence, the experimental study shows the necessity of implementing a decoupler between the adjacent zones, even though, the main objective of the study was to focus on the efficiency of optical fiber thermomemters (OTF) over conventional thermocouples. For the simplicity, similar to

the methods described above, each zone was equipped with an individual power supply which leads to control of temperatures in the zones individually. However, the coupling effect between the zones makes the control task difficult. Considering the fact that an accurate model facilitates the development of the efficient control of the temperature profile, a mathematical model was developed by the researchers taking into account environmental effect and all thermocoupling effects between zones. It was found that the state (temperature) at one zone was not only affected by the power source of that zone but also by the temperature of other zones. Hence, the decoupling controllers were introduced in the control system in order to compensate the thermocoupling effects between the neighbouring zones. The control structure of each zone consists of a main controller and two decoupling controllers for adjacent zones to compensate the thermocoupling effects. The minimal thermocoupling effects from the non-neighbouring zones were neglected. The block diagram of the controlled closed loop is shown in Figure 8 below. The left half (gray section) of the block diagram represents the furnace whereas the right half (dark section) represents the controllers.

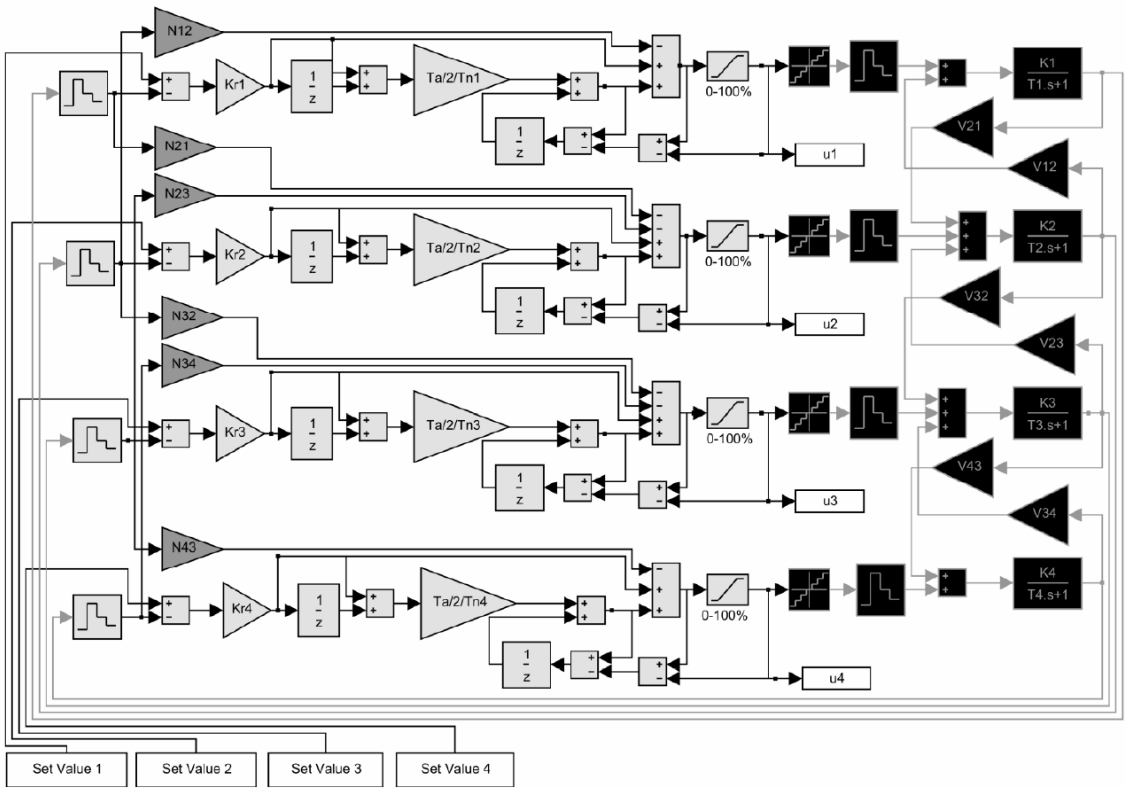


Figure 8: Block diagram of the controlled closed loop *(Sauermann , et al., 2001)*

The control performance of the furnace was tested up to 1500°C and the negligible deviation (about 0.02 °C) was noticed even at the maximum temperature. The research claimed that deviation was greater with the thermocouples,thereby confirming that OTF is superior to thermocouples in temperature sensitive control system.

Also, the research paper described the time constants of actuators(heating elements) of the zones. The study emphasized on the use of encapsulated graphite heaters (EGH) which has a very small thermal response time compared to the conventional heating furnace. Hence, the research concluded that choice of an appropriate temperature sensor (OTF), heating elements (EGH), and a controller (decoupling controller) leads to highly stable control of multizone furnaces.

## 4.2 Cascade Control Systems for the furnace

It has already been mentioned several times that a MHF or any other industrial furnaces possess complex and nonlinear characteristics. The control of the temperature profile using the conventional controller is not viable in a non-linear dynamical system. There are large delays in the multivariable system along with the cross-coupling relationship between the control variables. However, a certain section of an industrial furnace shows linear behavior, and thus, the conventional PI controllers can be efficiently applied. Considering, both linear and nonlinear characteristics in the furnace, few research studies have been performed using a cascade control system, where a conventional controller has been used for the control of the temperature in the furnace where it behaves linearly, whereas the advanced control system has been implemented on top of the conventional controllers for the control of temperature in the region of the furnace where it behaves non-linearly. A cascade control system is a system with multiple controllers where the controllers work in a hierarchy. The external (primary) controller works as the decisive (master) controller where control of the nonlinearly behaving region is carried out whereas the internal (secondary) controller works as a slave controller and controls the linearly behaving region of the furnace.

Moon & Lee(2000) studied the temperature control of the glass-melting furnace using a cascade control system. Similar to the furnaces mentioned before, temperature control in a glass-melting furnace is rather challenging due to the complex and non-linear characterstic

of the furnace. Despite the fact that the furnace posesses non-linear dynamics, some regions of the furnace behave linearly and hence can be modeled as a linear system. Although, a PI controller has proven to be easier to use and an effective controller for the linear systems, it does not perform satisfactorily for many non-linear systems. Hence, Moon & Lee(2000) combined the conventional PI controller and a fuzzy logic controller in a cascade to obtain the benefits of both controllers, which has proven to be an effective method in controlling the temperature profile of the glass-melting furnace. In particular, the PI controller was used for the linear part of the furnace ( crown region, assumed to control gas temperature) whereas the control of the non-linear region was done by a fuzzy logic controller ( bottom region, assumed to control solid temperature).

The glass furnace to be controlled consisted of two sections; melter and refiner. The melter consists of the upper and lower sections called regenerators used for the inflow of air and fuel for combustion and outflow of exhaust gases. The detailed description of the furnace is shown in Figure 9 below.

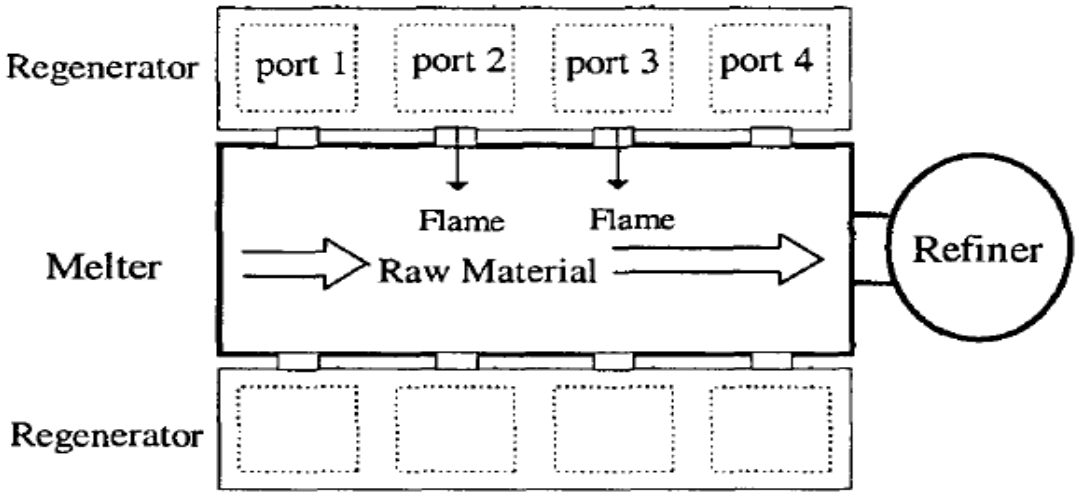


Figure 9: Simplified structure of the glass-melting furnace ( Moon & Lee, 2000)

The temperature of the furnace was controlled by observing the temperature at the crown(top) and the bottom of the melter and adjusting the fuel flow with respect to their values. The objective of the study performed by Moon & Lee(2000) was to maintain the glass temperature which is the bottom temperature of the melter. It was found out that a crown temperature has a quick response of the reaction rate on the fuel feed rate and disturbances, and its dynamics could be modeled with a linear first-order plus a dead time(FOPDT) model as shown in Equation 13. It can be controlled easily and effectively by

the conventional PID controller and hence, the PI controller (Equation 14) was designed based on the model. The PI controller was tuned to minimizes the integral of the time-weighted absolute value of the error (ITAE) to determine the gain (*Kp*) and the reset time ($\tau_i$).

$$G(s) = \frac{Y_c(s)}{U(s)} = \frac{Ke^{-Ts}}{\tau s+1} \tag{13}$$

$$G_c(s) = K_p(1 + \frac{1}{\tau_i s}) \quad where, K_p = \frac{0.859}{K}(\frac{T}{\tau})^{-0.977} \quad and\ \tau_i = \frac{\tau}{0.674}(\frac{T}{\tau})^{0.686} \tag{14}$$

Where, $Y_c$ is the crown temperature, *u* is the fuel, *K* is the steady gain, *T* is the process dead time, and τ is the time constant of the model.

However, the bottom temperature demonstrated the complex nonlinear behavior and time varying characteristics which make it difficult to model. The fuzzy rule base controller was thus used to control the bottom temperature of the furnace. The cascade controller proposed by Moon & Lee(2000) is shown in Figure 10 below. It is can be seen from the figure that input to the fuzzy controller is the bottom temperature deviation from a reference ($e_b$) and the change of the bottom temperature deviation ($\Delta e_b$) whereas the output has been used as the change in the set point of the crown temperature ($\Delta y_{sc}$).

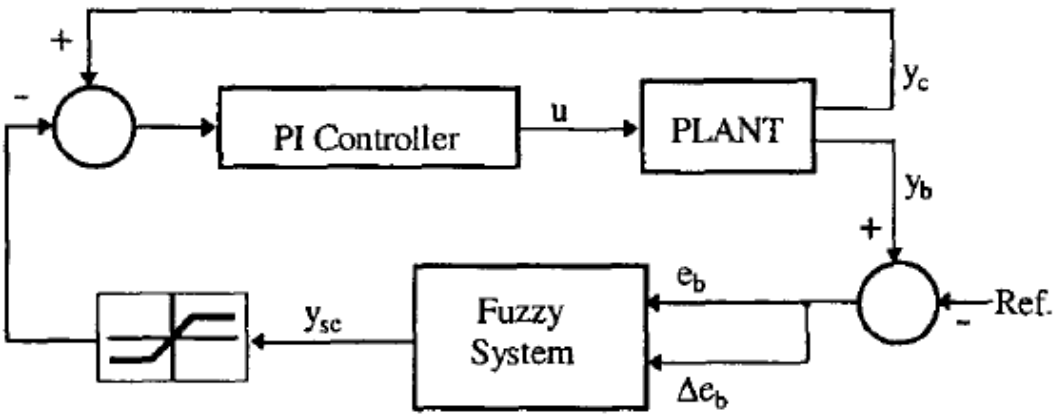


Figure 10: Cascaded fuzzy-PI controller for the glass-melting furnace ( Moon & Lee, 2000)

The input ($e_b$ and $\Delta e_b$) and the output ($\Delta y_{sc}$) of the fuzzy control system were divided into five (Negative Big (NB), Negative Medium (NM), Zero (ZO), Positive Medium (PM), Positive Big (PB)) and seven (Negative Big (NB), Negative Medium (NM), Negative small (NS), Zero (ZO), Positive Small (PS), Positive Medium (PM), Positive big (PB)) linguistic

expressions respectively and the fuzzy rule base set by the experience operators were implemented. The linguistic expressions were mapped as a membership function as shown in Figures 11-12, followed by the rule table depicted in Table 1.

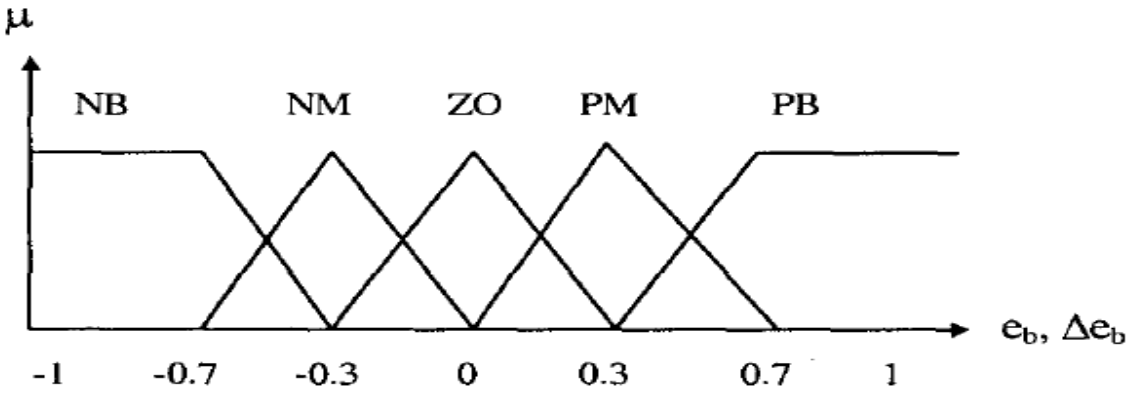


Figure 11: Membership function of input of the control system ( Moon & Lee, 2000)

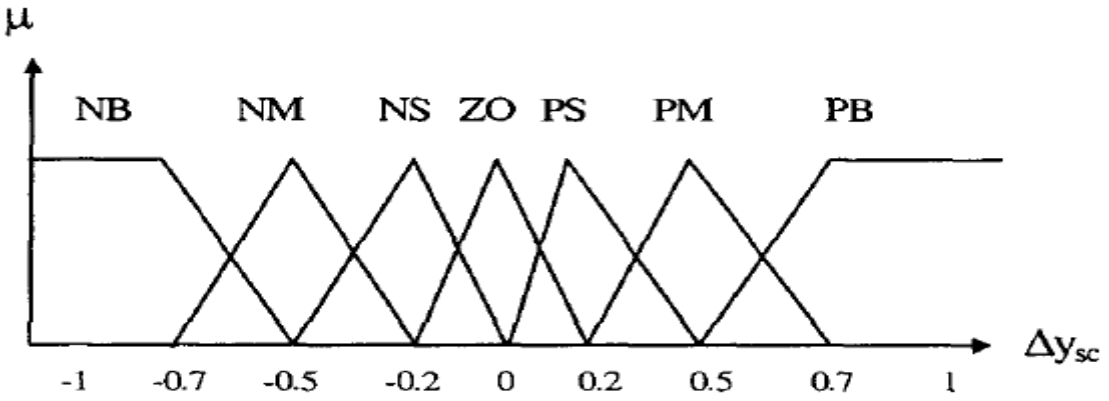


Figure 12: Membership function of output of the control system ( Moon & Lee, 2000)

Table 1: Rule table of the fuzzy system for the set point change in a crown temperature ( Moon & Lee, 2000)

| $\Delta e_b \setminus e_b$ | NB | NM | ZO | PM | PB |
|---|---|---|---|---|---|
| NB | PB | PB | PM | PM | PS |
| NM | PB | PM | PM | PS | PS |
| ZO | PM | ZO | ZO | ZO | NM |
| PM | NS | NS | NM | NM | NB |
| PB | NS | NM | NM | NB | NB |

The inputs $e_b$ and $\Delta e_b$ and the outputs $\Delta y_{sc}$ were scaled with the scaling factors $K_{eb}$, $K_{\Delta eb}$, and $K_{\Delta ysc}$ respectively. The scaled crisp inputs were then fuzzified with the singleton

fuzzification methods and the product inference was used. The truth-value and the output fuzzy set were calculated using Equations 15 and 16 respectively.

$$\omega_i = \mu_{A_i}(x) \cap \mu_{B_i}(y)|_{x=x_0, y=y_0} \tag{15}$$

$$\mu_C(z) = \cup_{i=1}^{m}\{\omega_i . \mu_{C_i}(z)\}, \tag{16}$$

where $\omega_i$ represents the truth-value of the *i*-th rule, $\mu_A(x)$ , $\mu_B(y)$, and $\mu_C(z)$ are the membership functions of the fuzzy sets of the inputs and output respectively, A and B are the fuzzy sets of inputs, x and y are the variables $e_b$ and $\Delta e_b$ , $\cap$ and $\cup$ are the minimum and maximum operator, m is the number of rules, and $x_0$ & $y_0$ are the crisp units at the k-th sampling step explained in Equations 17-18 below.

$$x_0 = K_{eb} e_b(k) \tag{17}$$

$$y_0 = K_{\Delta eb} \Delta e_b(k) \tag{18}$$

And the center of the gravity defuzzification method was used to obtain the control crisp output which is given by,

$$z_0 = \frac{\int z\, \mu_C(z) dz}{\int \mu_C(z) dz}, \tag{19}$$

where $z_0$ is the crisp output of the fuzzy inference.

On scaling with a scale factor $\Delta y_{sc}(k+1) = K_{\Delta ysc} Z_0$ , we get the output of the fuzzy system as,

$$y_{sc}(k+1) = \Delta y_{sc}(k+1) + y_{sc}(k) \tag{20}$$

On implementation to the industrial environment, it was found out that the fuzzy-PI based cascade controller was able to operate smoothly with negligible temperature variation. The experiment was conducted for a week and it was found that a variation range to the set point was within $\pm 0.5$ ℃ with standard deviation 0.23 ensuring the efficient temperature control of the furnace.

Doane (1968) patented a method to control the temperature in a multi-zone heat exchanger using the temperature sensing devices. The control method proposed is a cascaded control system where the slave controller controlled the temperature in the individual zone and all slave controllers were controlled by the external master controller. The control system consists of three slave controllers for each zone, one master controller, and a uniform temperature block in between slave controllers and a master controller which work as an

intermediate controller. The temperature in each zone of the heat exchange system was controlled by implementing the slave controller (secondary controller) in each zone where the controller controls the temperature in each zone by controlling the heating units available in each zone. A uniform temperature block (intermediate controller) located in between the master controller and the slave controller control the slave controllers as per the instruction of the master controller.

All four zones and the uniform temperature block were equipped with heating devices and thermocouple sensing devices. Also, the slave controllers have a reference temperature sensing devices in the uniform temperature block. The slave controllers were initially set to the desired temperature in each zone individually but get updated on any change in the uniform temperature block. The change in temperature in the uniform temperature block was transmitted to each slave controller by the reference temperature sensing element. Hence, the temperature could be changed at once and equally in all the zones via the master controller.

Whenever the temperature needs to be changed in the system, the uniform temperature block was changed by the master controller activating the heating devices of the uniform temperature block which eventually changes the temperature in the slave controller resulting in the change in the temperature of the furnace. The reference temperature sensing elements used were either thermocouple junctions or resistance members of a Wheatstone bridge. Also, it was mentioned in the patent that it is wiser to use a temperature program controller for any system where the temperature needs to be updated regularly in a specific time-range by the predetermined value as well as to the system where the temperature gradient should be established over the length of the system.

## 4.3 Model predictive control of the furnace

Model predictive control (MPC) is an advanced control method widely used in industries for tcontrol of the multivariable systems. MPC has been considered suitable for the complex industrial applications due to the fact that it can handle complex characteristics of the system, such as multivariable process interactions, time delays, input/output constraints, various measurable and unmeasurable disturbances. Further, it can handle various other complication occurring due to non-linear behavior of the system. The model predictive

controller works on the pinciple that , it utilizes the dynamic model of the process to predict the future output at subsequent time horizon and then uses the same model to calculate the future control sequence minimizing the specified optimization objective under specified constraints. The predicted future output is compared with the plant measurement and thus future predictions are updated based on an obtained error. In summary, the future output of the plant is predicted using the model, the past and current data, and calculated future control actions. Since MPC is best practiced in the multivariable systems having interactions between single output single input (SISO) loops, the implementation of it in MHF is favorable. There are numerous past studies on controlling the temperature profile in the furnace using MPC algorithm, few of them are discussed in this thesis work.

Stadler, et al.(2011) introduced the model predictive controller to maintain the desired temperature profile of a rotary cement kiln. Since, the quality of the cement produced heavily depends on the quality of clinker, the semi-processed product formed during cement formation, it is of great importance to maintain the temperature profile in the kiln during clinker formation. Another variable that can change the quality of clinker is oxygen level as it determines fuel combustion and hence, needs to be controlled. The whole clinker production process in the kiln can be generally categorized into four sub-processes; preheating, calcination, sintering, and cooling. The researchers divided the process into five zones (compartments) based on the sub-processes, where the transition zone was inserted in between the calcination and sintering.

The thermodynamic behavior of the clinker formation in the kiln was modeled considering the heat transfer in rotary kilns to be generally via radiation and a combination of convection and conduction. The model built considered the heat transfer via convection and radiation. The division of the process into five zones facilitated overall thermodynamic modeling of the process. Figure 13 illustrates the sub-processes (where the major chemical reaction takes place) as well as five compartments of the process along with the temperature profile of the feed and gas along the process. However, temperature profile shown in the figure cannot be measured due to the unavailability of the temperature sensors along the rotary kiln, and thus, temperature profile estimation needs to be considered while designing the model.

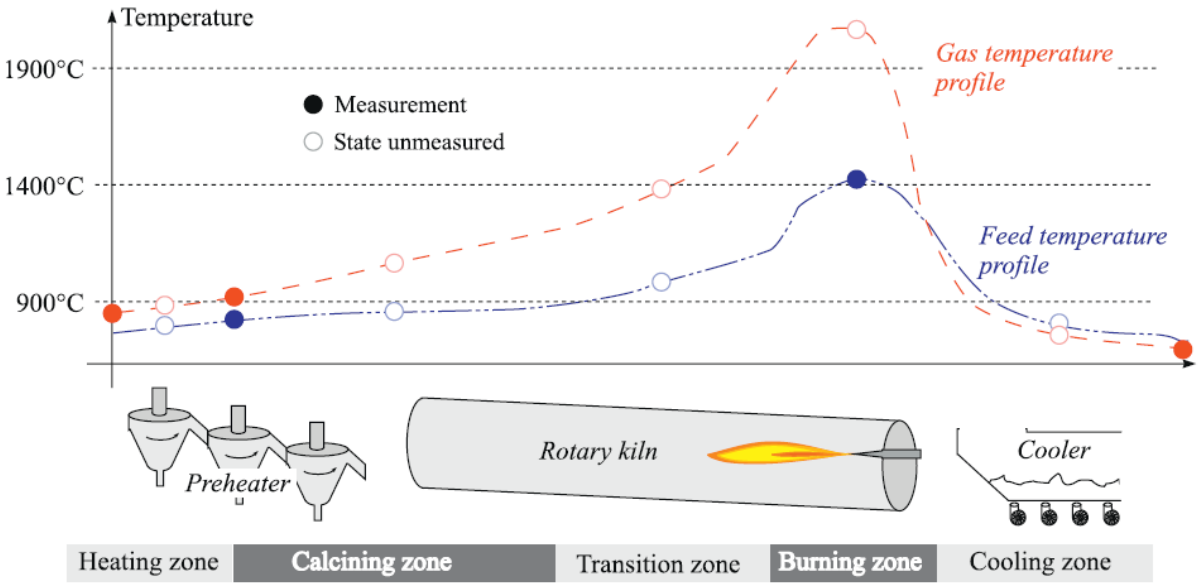


Figure 13: Kaolin diagram representing the temperature profile along the kiln and categorization of the kiln into zones ( Stadler , et al., 2011)

The thermodynamic behavior of the zones was described by a mass and energy balance. As the energy transfer in the system is related to feed and gas transport, fuel combustions, environment, and chemical reactions, the following model equations of mass transport dynamics, feed and gas temperature dynamics, and oxygen dynamics were used with few assumptions. The state, input, and parameters of the model are represented in Table 2.

Mass transport dynamics is as follows:

$$m_i{}^f = \frac{1}{L_i}(u_i{}^{fin} - m_i{}^f . u_i{}^v) \tag{21}$$

Feed temperature dynamics is,

$$c^f m_i{}^f T_i{}^f = \frac{c^f u_i{}^{fin}}{L_i}\left(u_i{}^{T_{fin}} - T_i{}^f\right) + k_i{}^t\left(T_i{}^g - T_i{}^f\right) + \frac{u_i{}^v m_i{}^f k_i{}^c}{L_i} - \frac{k_i{}^l T_i{}^f}{L_i} \tag{22}$$

Gas temperature dynamics is,

$$c^g m^g T_i{}^g = \frac{c^g u^{g_{flow}}}{L_i}(u_i{}^{T_{gin}} - T_i{}^g) - \left(T_i{}^g - T_i{}^f\right) + \frac{1}{L_i} u_i{}^{fuel} \tag{23}$$

Oxygen dynamics is described by the following equation:

$$\dot{O} = a^{oxy} O + k^{oxy} u^{g_{flow}} - c^{oxy} u^{fuel}, \tag{24}$$

where $i$ = 1,2,3,4, and 5 is the zone in the kiln process, $(\dot{O})$ is the oxygen content in the exhaust gas, $a^{oxy}$ describes the sensor dynamics, $k^{oxy}$ and $c^{oxy}$ describes oxygen source and sink.

Table 2: State, input, and parameters of the model ( Stadler , et al., 2011)

| Zone State | Zone input | Zone parameters |
|---|---|---|
| Average mass density ($m_i{}^f$)<br>Feed temperature ($T_i{}^f$)<br>Gas temperature ($T_i{}^g$)<br>Oxygen content in the exhaust gas ($\dot{O}$) | Feed transport velocity ($u_i{}^v$)<br>Energy released by burning fuels ($u_i{}^{fuel}$)<br>Gas flow ($u^{g_{flow}}$)<br>Feed input ($u_i{}^{fin}$)<br>Input feed temperature ($u_i{}^{T_{fin}}$)<br>Input gas temperature ($u_i{}^{T_{gin}}$) | Compartment length ($L_i$)<br>Specific heat capacity of meal feed ($c^f$)<br>Specific heat capacity of gas or air ($c^g$)<br>Average mass density of gas or air state ($m^g$)<br>Energy loss in the compartment ($k_i{}^l$)<br>Energy source (+) or sink (-) due to chemical reaction ($k_i{}^c$)<br>Heat transfer coefficient between gas and feed state ($k_i{}^t$) |

As the controller proposed by the researchers was only compatible to linear models and the model should be simple enough to be implemented, the nonlinear model formed above was linearized. The proposed model has the following states in each zone; average mass density, feed temperature, and gas temperature and an oxygen state. However, all the measurements are not available, and hence, moving horizon estimation (MHE) was used to determine the current state and to implement model predictive control (MPC). MHE problem formulated as given in Equation 25.

$$\min_{x} \ \sum_{K=-N}^{-1}\{||y^{obs}[k] - (Cx[k] + Du[k])||_R^2, + ||x[k+1 - A(x[k] + Bu[k])||_Q^2\} \tag{25}$$

subject to $\quad Sx[k+1] = S(Ax[k] + Bu[k])$

$$-E_5 = E_4 x[k + E_1 u[k],$$

where A, B, C, and D are the matrices of the system, *x[k]* is the state vector, $E_x$ are the constraints, *R* and *Q* are the weight matrices for the measurement error and the dynamic error. A matrix S is used to enforce state evolution for certain states.

The MHE problem formulated was further reduced to make the estimator more robust. The optimal control problem was then formulated in a standard way as shown below in Equation 26.

$$\min_{x,u,z} \sum_{K=0}^{M-1}\{||y^{ref}[k] - (Cx[k] + Du[k])||_{W}^{2}, .. + L(Cx[k] + Du[k]) + ||z||_{W_z}^{2} + L_z z[k]\} \tag{26}$$

subject to $x[k+1] = Ax[k] + Bu[k]$

$x[0] = x^{start}$

$E_3 z[k] = E_4 x[k + E_1 u[k] + E_5,$

where *M* is the receding control horizon. *W, L, W*$_z$, and $L_z$ are the quadratic and linear costs of states and auxiliary variables respectively, z is the auxiliary variables that defines soft constraints.

The controller designed based on the model of the system was then implemented in a cement plant. The major process variables controlled are the burning zone temperature (BZT), the back end temperature (BET), and oxygen after combustion and the manipulated variables are feed rate and the specific energy input(SpecE). The reference range of the process variables was implemented as the soft constraints in the controller. The controller was able to keep the burning zone temperature within the desired range thus ensuring the better quality in the clinker. Also, along with the BZT, other variables were also kept within the desired range even though significant external influences in the process was noticed during the implementation. Figure 14 illustrates the variation in a burning zone temperature with the manual control and the proposed model predictive control. It can be clearly seen from the plot that, the variation in the BZT has been greatly reduced during the time MPC has been used (second half of the plot), thus ensuring the better control of temperature in the burning zone. Also, the MPC controller showed the better feed rate and lower specific energy consumption.

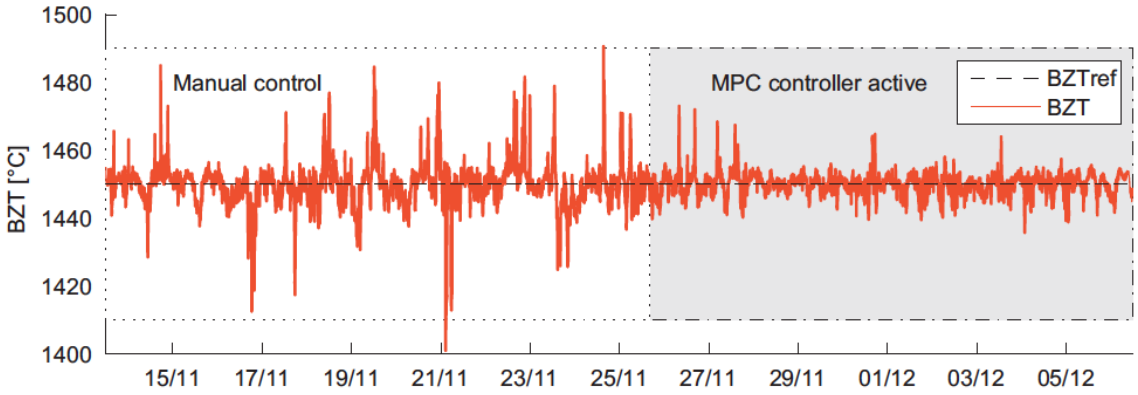


Figure 14: Burning zone temperature(BZT) and its reference(BZTref) on manual control and the MPC controller ( Stadler , et al., 2011)

Valiquette, et al. (1997) studied the practical aspects on the implementation of MPC on an industrial lime kiln. The lime kiln was used for the kraft recovery and caustizing operation during the kraft pulping process. Since, temperature profile along the kiln is an important factor that determines the quality of the lime and its granular size, controlling of it is fundamental in order to obtain lime of high quality. As mentioned in the previous research studies, maintaining of oxygen level in the flue gas is also quite important for complete combustion. It is also an important factor to consider regarding energy efficiency, refractory wear, and environmental emissions . However, it is difficult to control the kiln as it is a nonlinear multivariable process with disturbances and strong interaction between varaiables. Conventional PID controllers traditionally used for the control of kiln were unable to precisely control the temperature profile along the kiln due to the strong interactions.The addition of dynamic decouplers has been successfully used to cancel out the interaction between the loops, the controllers still lack the ability to handle large delays and constraints . Also, the tuning and maintenance of the decoupled PID controllers are difficult. Hence, a model predictive control with input and output constraints was implemented to maintain the desired temperature profile along the kiln as well as the oxygen level.

The main objective of the research study was to control the temperature profile along the kiln for proper calcination of lime by controlling the temperature of the kiln at two ends. The feed end temperature and discharge end temperature were controlled by manipulating the fuel flow rate and the induced draft (ID) fan. Also, the excess oxygen was measured at the feed end to maintain the oxygen level. The identification experiments were carried out based on pseudorandom binary sequences (PRBS) to obtain the model of the system. The

experiments were based on the step response tests and process knowledge. In order to obtain an accurate model, the experiment was carried out in a disturbance free period and manipulating single variable at a time. The impulse response model was formed to predict the future response of the process and the prediction was used to minimize the sum of squared errors. The optimal control problem was then formulated incorporating the constraints. The algorithm formulated is shown in Equation 27.

$$\min_{\Delta U(k)} \{\sum_{K=1}^{p} ||\Gamma^{y}\,[Y(k+1|k) - R(k+1)]||^2 + \sum_{K=1}^{m} ||\Gamma^{u}\,\Delta U(k)||^2\}, \quad (27)$$

Subject to

$$Y \le Y(k+1|k) \le \bar{Y}$$

$$U \le U(k+1|k) \le \bar{U}$$

$$\Delta U \le \Delta U(k+1|k) \le \overline{\Delta U}$$

For k =1, 2, 3… p

where *p* and *m* are the prediction and control horizon respectively. $\Gamma^{y}$ and $\Gamma^{u}$ are the tuning parameters of the controlled and manipulated variables respectively.

The controller designed was then implemented in the lime kiln to maintain the temperature profile and oxygen level of the kiln. It was found that MPC was able to control the temperature profile along the kiln maintaining the oxygen level within the set constraints. The variation in the temperature was found to be within 5 ℃ and 10 ℃ at the feed end and discharge end respectively when the MPC controller was used, which reveals better control in temperature compared to the conventional PID controller where the variation was up to 20 ℃ and 50 ℃ at the feed end and discharge end respectively.

Figure 15 illustrates the response of the control variables and manipulated variables. The results shown reveals the steady controlled and manipulated variables. The controller was able to handle minor disturbances however, there was an interruption on lime mud feed for thirty minutes at time three hours and the disturbances can be noticed clearly in the plots. The feed end temperature (FET) was disturbed as the supply of mud was stopped, however, the major disturbances on the discharge end temperature (DET) were seen just after the operation was resumed after an interruption as the thin layer of lime formed absorb more heat. Since the pyrometer reading is affected by the dust and flame, the second order Butterworth filter was used to reduce the effect. Also, the pyrometer was cleaned (sudden

variation is seen in DET plot) during operation to study the disturbances effect, which controller was able to deal with. The oxygen level was maintained with the constraints limit set.

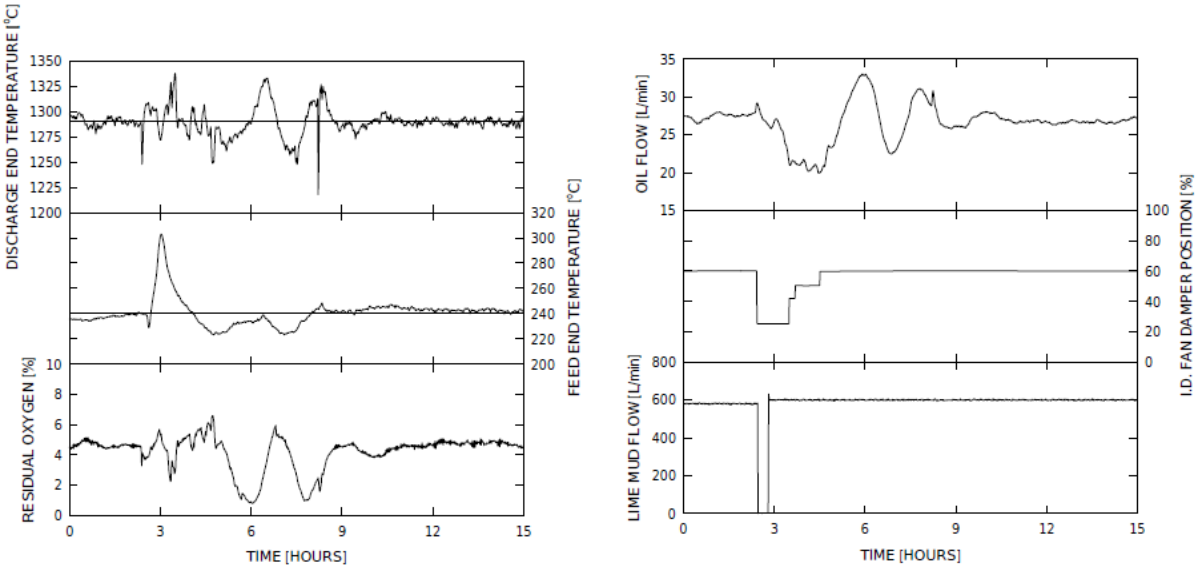


Figure 15: Controlled variables response and manipulated variables response of the lime kiln control using MPC (Valiquette, et al., 1997)

## 4.4 Other advance control strategies for temperature profile control

Besides above mentioned control methods, various other control strategies have been implemented to maintain the desired temperature profile along the furnace/kiln/oven in the mineral and process industries. Few of them are discussed in this work.

### 4.4.1 Multivariate controller

Akalp, et al. (1994) performed a research study on a rotary cement kiln. The main objective of their study was to develop a control method to maintain the desired temperature profile in the kiln as the quality of cement produced depends on the temperature in the kiln. However, the control of temperature in the kiln is complicated due to its time-varying nonlinear behavior and large dimensionality of the problem. Controlling the temperature in the kiln requires manipulation and control of many variables. Hence, they proposed the fuzzy based multivariate controller to maintain the desired temperature profile in the kiln. The important

variables used for the control purposes are demonstrated in the schematic diagram of rotary cement kiln (Figure 16).

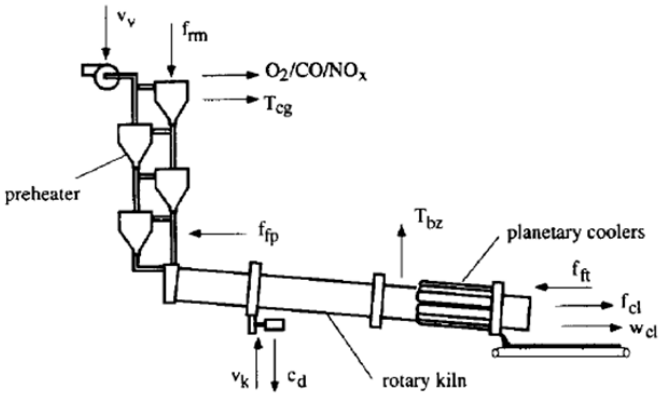


| Control Variables | Output Variables |
|---|---|
| Feed rate of raw mix ($f_{rm}$)<br>Fuel feed rate at twyer ($f_{ft}$)<br>Fuel feed rate for precalcination ($f_{fp}$)<br>Rotation kiln speed (($V_k$)<br>Ventilator speed ($V_v$)<br>Burning zone temperature ($T_{bz}$)<br>Combustion gases temperature ($T_{cg}$)<br>O2/CO/NOx contents of combustion gases<br>Kiln drive power($C_d$) | Feed rate of clinker ($f_{cl}$)<br>Clinker liter weight ($w_{cl}$) |

Figure 16: Schematic diagram of the rotary kiln (Akalp, et al., 1994)

Akalp, et al. (1994) conducted their study by controlling the temperature at two important points in the kiln; calcining zone ($T_{cg}$) and burning zone ($T_{bz}$) using fuzzy based multivariate controllers . Three fuzzy logic controllers were implemented with the controlled variables $T_{cg}$ , $T_{bz}$ , $C_d$ , $f_{rm}$, $v_k$ and $f_{ft}$. The schematic diagram of the proposed controllers is shown in Figure 17 below.

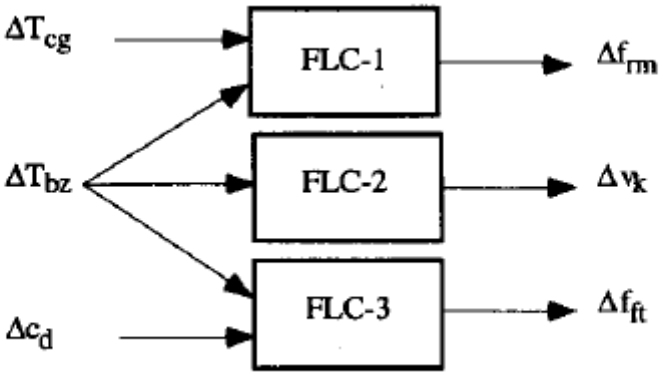


Figure 17: Proposed controllers for a rotary cement kiln (Akalp, et al., 1994)

Figure 17, depicts that the control error on combustion gas temperature ($\Delta T_{cg}$) and burning zone temperature ($\Delta T_{bz}$) were used as an input to the controller FLC-1, $\Delta T_{bz}$ was used as an input to the controller FLC-2 , and $\Delta T_{bz}$ and $\Delta C_d$ were taken as an input to the controller FLC-3. The inputs and outputs were categorized into different sections based on fuzzy linguistic expressions, which were mapped as membership functions. The fuzzy based rule developed by the operator were implemented in the membership functions, which on

fuzzification yields the output fuzzy set. The example membership functions for input $\Delta T_{cg}$ and $\Delta T_{bz}$, and the output $\Delta f_{rm}$ are presented in Figure 18 followed by the table of a set of 15 fuzzy based rules.

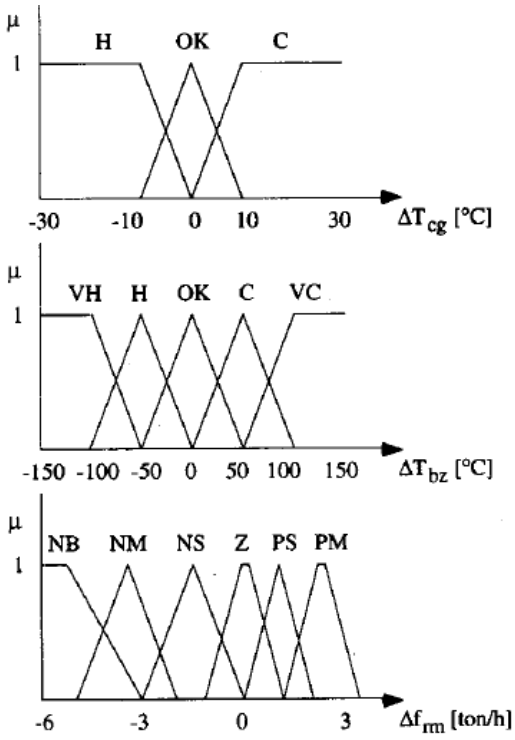


| $\Delta T_{cg}$ \ $\Delta T_{bz}$ | VH | H | OK | C | VC |
|---|---|---|---|---|---|
| H | PM | PM | Z | NS | NB |
| OK | PM | PS | Z | NM | NB |
| C | PS | Z | Z | NM | NB |

Fuzzy linguistic expressions

Very Hot (VH), Hot (H), Okay (OK), Cold (C), Very Cold (VC)

Negative Big (NB), Negative Medium (NM), Negative small (NS), Zero (ZO), Positive Small (PS), Positive Medium (PM)

Figure 18. Membership function for input and output as well as the associative memory for FLC-1 (Akalp, et al., 1994)

The obtain output $\Delta f_{rm}$ , $\Delta V_k$ , and $\Delta f_{ft}$ were added to the prior value of $f_{rm}$, $V_k$ and $f_{ft}$ to get the optimized value. Initial $f_{rm}$ and $f_{ft}$ were the desired set point value chosen by the operator whereas $v_k$ was determined as a function of $f_{rm}$ to maintain the flow of raw mix. Since the control on combustion gas temperature can be achieved by the action on $f_{rm}$ , optimized $f_{rm}$ leads to controlled combustion gases temperature. Similarly, optimized , $f_{rm}$, $v_k$ and $f_{ft}$ leads to the controlled burning zone temperature whereas the kiln drive power is controlled due to the fact that it provides the internal state (burning condition) of the kiln. Figure 19 below shows the variation in a variable due to other controlled variables . Hence, the results revealed that various other variables need to be controlled to maintain the desired temperature profile in an industrial process.

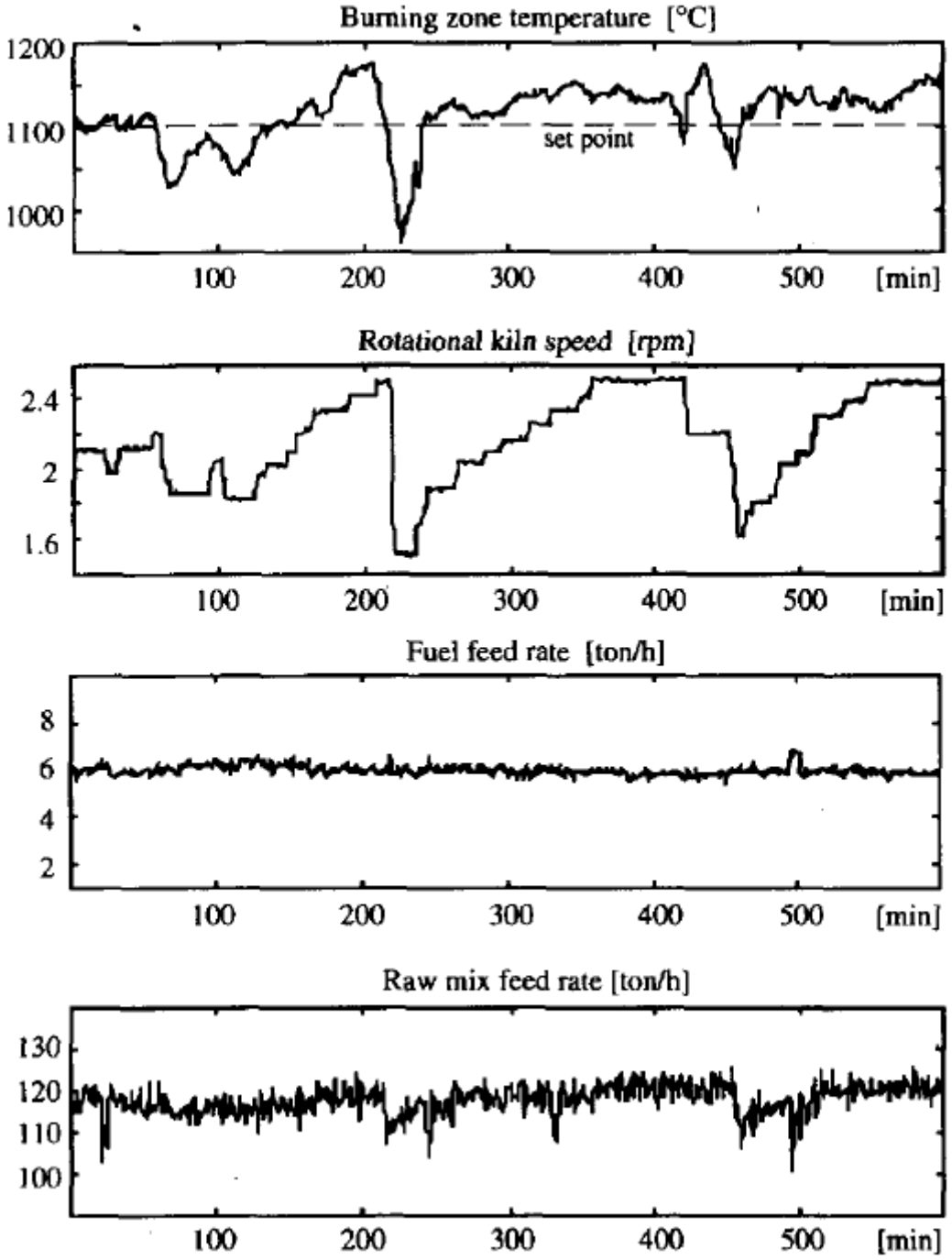


Figure 19: Variation in each variable due to the effect of other variables (Akalp, et al., 1994)

### 4.4.2 Zone control

Temperature not only varies between the zones but also remains non-uniform within the zone in the multi-zone furnace/kiln. Varies control methods have been implemented to

maintain the uniform temperature within the zone. Automated Zone control technology has emerged as a relevant control mechanism in an industrial furnace/kiln. The method has proven its potential in maintaining the uniform room temperature in heating, ventilation, and air-conditioning (HVAC). The method has now been implemented in an industrial ceramic electrical kiln to maintain the uniformity in temperature at the top and bottom of the kiln. Figure 20 illustrates the variation in temperature within the zone (top and bottom of the zone) in a three-zone kiln, which is controlled to achieve the desired temperature by the implementation of automated zone control. Automated zone control systems have become more convenient as it allows dynamic adjustment as well as the introduction of bias in the zone. The automated zone control design has been thus, considered as a relevant option in a multi-zone operation due to its ability in maintaining the desired temperature of each zone independently in a separate control loop. (LL Kilns, 2010)

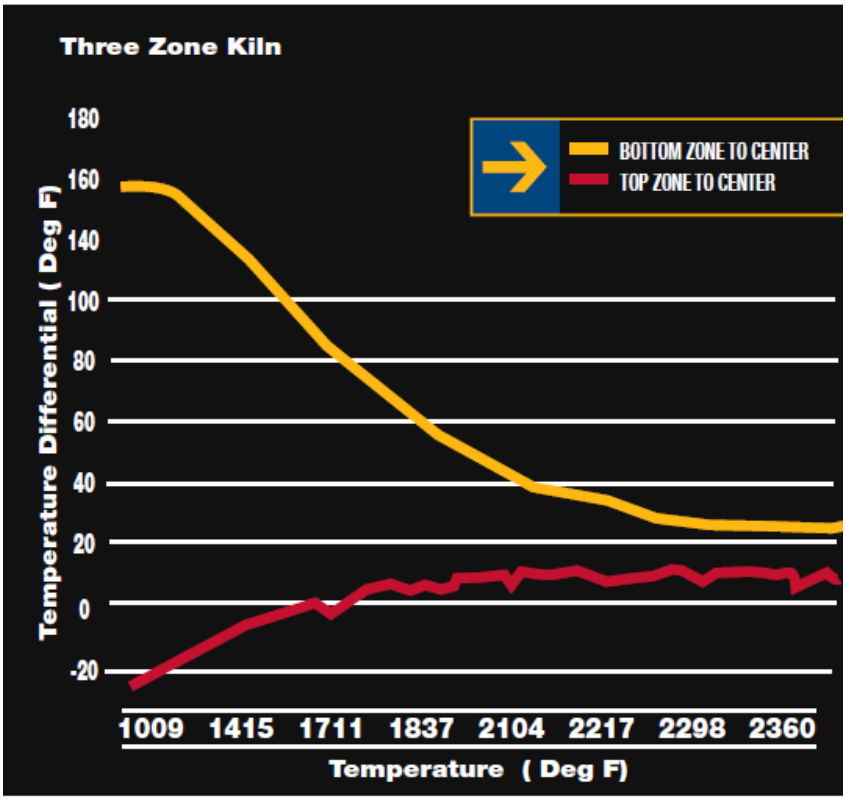


Figure 20: Temperature control in a kiln by zone control systems (LL Kilns, 2010)

### 4.4.3 Control of temperature with Mist

McIntyre,et al. (1991) patented a method to control the temperature in the combustion zone of MHF and fluidized bed furnace (FBF) with the use of a carrier gas. The invention describes the process of controlling the furnace temperature without supplying additional

cooling air. The furnace was facilitated by the several ports (multiple in each zone) with low volume gas entry to the combustion zone from where the carrier gas was supplied. Fine water mist generated by the two-fluid atomizer was present in the carrier gas, which absorbs heat from the combustion zone by evaporation. The furnace was equipped with the controller that controls the water supply to form the mist. The controller opens the water valve to form mist when the temperature sensor in the combustion zone crosses the desired set point and thus the mist is sprayed into the combustion zone to reduce the temperature in the zone. The use of mist instead of water was found to be prominent due to the fact that furnace could be damaged by the direct use of water.

The patent also discusses about the previously patented and implemented temperature control methods in furnace, such as supplying of air to individual hearth in order to add an oxidant, circulation of low temperature gases from drying zone to the combustion zone to absorb the excess heat from combustion zone, and supply of high velocity mixing jets to combustion hearths.

# 5. Aim of the experimental part

The aim of the experimental part is to propose a new control strategy scheme for the multiple hearth furnace. Since the stability of temperature in the furnace determines the quality of the end product, maintaining of it is crucial. Various ore properties (e.g., particle size distribution, structure ordering and some impurities) strongly affect the heat of reactions and reaction rates, thereby shifting the temperature profile in the furnace and thus changing the properties of final product.

As it is difficult to measure the product characteristics and the solid temperature in the furnace online, the existing control system mostly attempts to maintain the constant gas temperature using traditional control implementations, such as PIDs. However, it is practically impossible to stabilize the whole gas temperature profile in the studied furnace, since there are not enough actuators (burners) available in the furnace. Thus, only the gas temperatures in hearths 4 and 6 are controlled. This strategy helps to attenuate the variations in the solid phase temperature and the calcination reaction rates throughout the furnace. However, the variations in the solid phase are not eliminated completely due to presence of varying ore types and mineralogy, and therefore, this strategy does not allow achieving the uniform product calcination.

In the experiment, the analysis based on historical data is conducted to study the major process disturbances, and their relations to the process phenomena of the furnace. To cope with the disturbances related to the varying ore properties, a new control strategy needs to be developed. When developing the control strategy for the MHF, energy balance needs to be taken into consideration as it plays a key role. Hence, this thesis aims at developing the soft sensor based on energy balance to estimate the exothermic reaction rate in the hearth 4.

# 6. Description of the multiple hearth furnace and its current control strategy

This section includes the description of the multiple hearth furnace, a system considered for this experimental study. The multiple hearth furnace is a Herreschoff calciner consisting of eight hearths constructed of bricks. The schematic diagram of the MHF is shown in Figure 21. Total eight burners are located in the hearths four and six for the supply of heat required in the furnace, four burners are tangentially placed in each hearth. The kaolin fed from the top of MHF is moved by the rabble arms and is dropped downward via holes located in the center of the odd numbered hearths and periphery of the even numbered hearth. Calcined material is collected from the two discharged holes located at the bottom of the furnace. The residence time of the feed in the MHF can be controlled by adjusting the rotational speed of the central shaft. On the contrary, the exhaust gas formed by the combustion of methane gas in the hearths 4 and 6 moves in the upward direction and exits from the top of the furnace (Mcketta & Cunningham, 1978, Hennion, 1987). The heat transfer to the feed originates primarily from the gas phase and through the radiation from the hearth walls.

The temperature in the hearths 1-6 increase gradually but the temperature in hearths 7-8 decrease as the calcined material cool down in these hearths. The dewatering of kaolin feed and transformation of kaolin into metakaolin occurs in the hearths 1-5, whereas the crystalline spinel phase formation takes place at the temperature of about 930 ℃-1000 ℃. The energy released by the burners placed in the hearth 4 is primarily used for heating the kaolin from 30 ℃ to a higher temperature (at least 450 ℃) at which it undergoes dehydroxylation reaction. The energy released by the burners in the hearth 6 is mainly used for increasing the temperature of metakaolin sufficiently enough for converting it to the spinel phase. The solids reach the highest temperature in the hearth 6, and hence the control of it is essential to ensure the product is at the desired temperature range and that overheating of the product has not occurred. The calcined kaolin starts to cool down in the hearth 7 and the cooling process is also continued in the hearth 8 until solids leave the furnace via discharge holes. Even though MHF is easy to operate and to maintain, long startup and shutdown time restrict its use only for continuous operation (Sell, 1992). The estimated temperature profile of a MHF is also shown in Figure 21 (Thomas, 2010, Eskelinen, 2014).

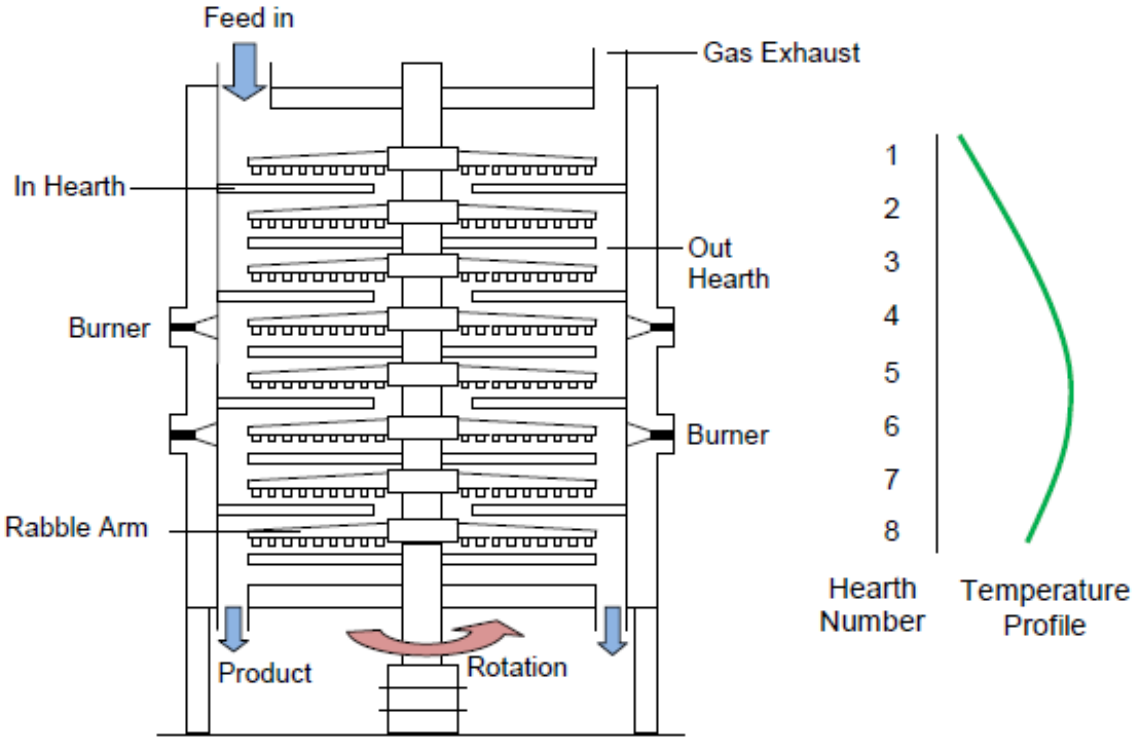


Figure 21: Schematic diagram of the Herreschoff multiple hearth furnace and the estimated temperature profile (Thomas, 2010):

Controlling the temperature profile is critical in kaolin calcination to obtain the end product of the desired specification. The feed rate, the rotational speed of the shaft and the rabble arms, and the orientation of the teeth on the rabble arms are important parameters affecting the temperature profile of the MHF in addition to the ore mineralogy. However, the temperature profile of kaolin along the furnace is mainly driven by the gas phase temperature in the MHF. Hence, controlling the gas phase temperature is imperative in obtaining the desired product quality.

Currently, in the hearth 4 the gas temperature in each burner is controlled by the PI controller, as shown in Figure 22.

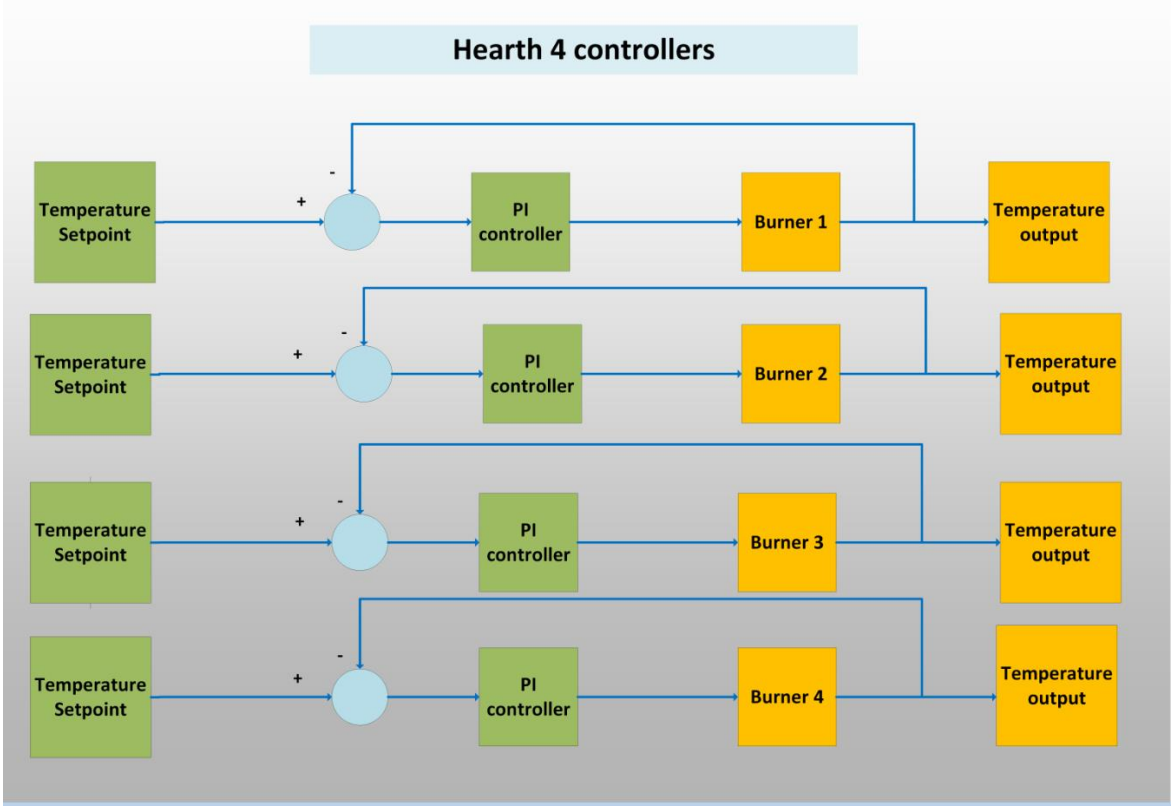


Figure 22: PI controller for each burner in the hearth 4

The set points for hearth 4 and hearth 6 temperature (gas burners) are provided by the operators along with the set points for feed rate and rotational shaft speed as they have direct impact on temperature profile of kaolin, which ultimately affect the brightness and particle size of the end product. The gas temperature in each burner is then controlled by the PI controller.

In the furnace under study, it was found out (from the process data) that the controllers do not behave optimally in all the process conditions under the current control strategy. For example, from Figure 23 obtained from real process data, it can be seen that only one controller follows the temperature set point at a time, while other temperature measurements deviate up to 50 °C from the set point during the whole operation. Also, the gas flow behaves in a similar manner, where one burner is found to be actively operating while the rest remain at maximum limit as shown in Figure 24. The variation in the temperatures in the hearth 4 was also studied by Gómez Fuentes (2016). According to Fuentes, the variation in the temperature occurred due to input (gas flow to a burner) saturation. The saturation effect can be caused by a high furnace capacity exceeding its maximum design value and also by tangential placement of the burners which creates coupling between them (one burner

hinders the gas flow of the other). The actual process data obtained from the plant have been normalized due to confidentiality. Hence, the all the figures plotted have normalized data.

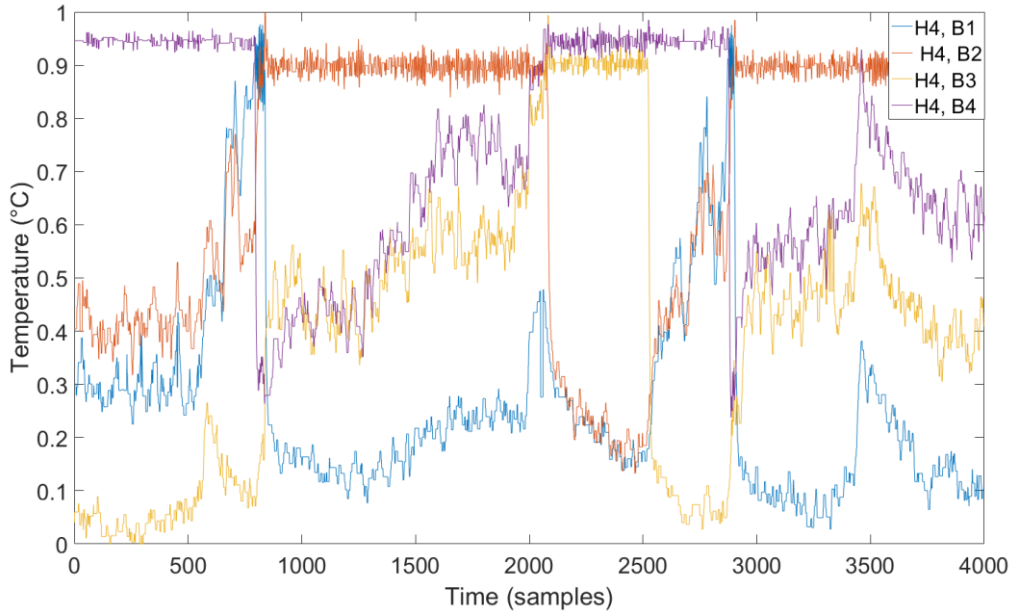


Figure 23: Temperature behavior of the gas flow in the hearth 4 (Real process data)

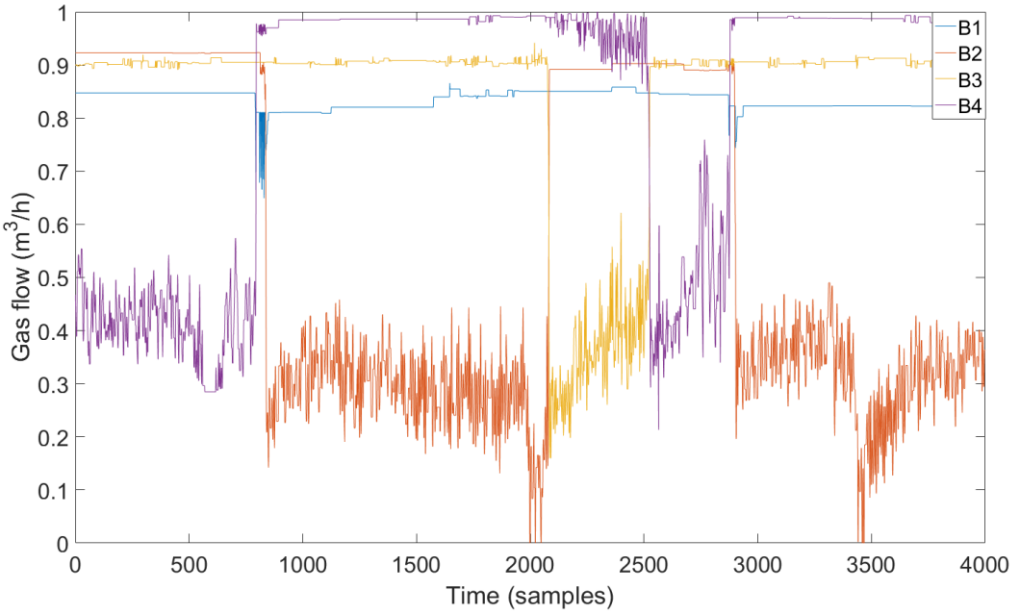


Figure 24: Gas flow in the hearth 4 (Real process data)

In a similar manner to the hearth 4, the basic PI controllers are used to control the gas temperature in hearth 6. Since, the quality of end product is considered to be mostly dependent on the temperature in the hearth 6, it is operated almost to the set point temperature. It can be seen that all the four temperature measurements follow the set point

given by the operator with the maximum variation of about 5 °C. However, the gas flow varies greatly to keep the temperature in the hearth 6 to the set point value.

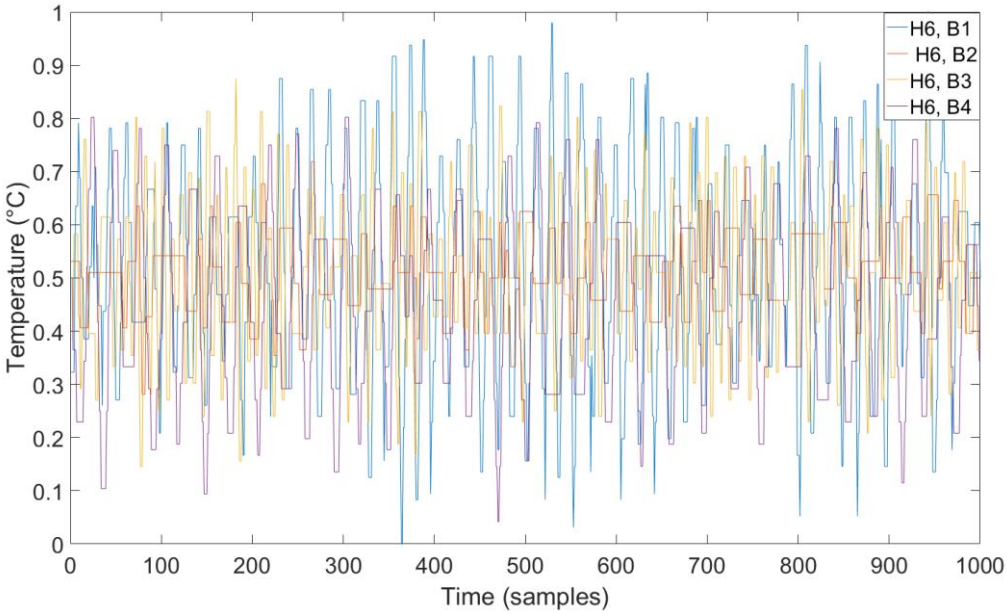


Figure 25: Temperature behavior of gas in the hearth 6 (Real process data)

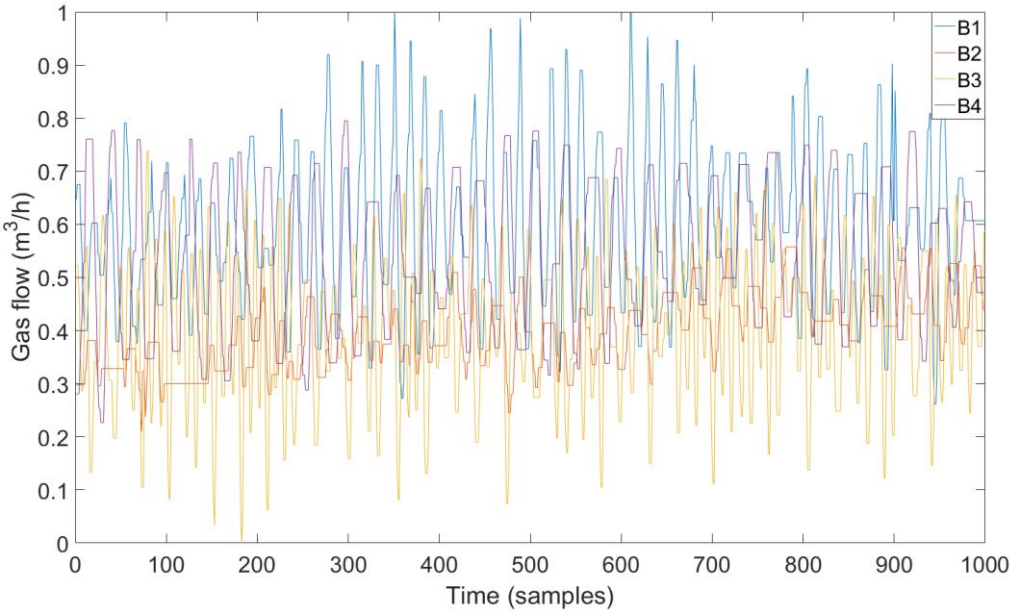


Figure 26: Gas flow in the hearth 6 (Real process data)

# 7. Data-based analysis of the operating conditions in the furnace

The data analysis presented in this section aims to study the variations in the process and their effects on the operating conditions of the furnace. The analysis is performed separately for the upper (top 5 hearths) and the lower (bottom 4 hearths) sections of the furnace. Historical data for the study was collected from the real process from the beginning of May to the end of November 2013 (7 months) with the time interval of 30 seconds and the study is focused on the process behavior, where the temperature and the behavior of fuel consumption were analyzed considering the variations in the process.

## 7.1 Analysis of the hearths 1 -5

First, the upper section of the furnace (hearths1-5) was analyzed focusing primarily on the behavior of the temperature measurements in the hearth 4 and 5. During the data visualization, many examples were found where the temperatures in the hearths 4 and 5 were very low while the gas flow to the hearth 4 was at its maximum, the cases are provided in Figures 27 and 28. From the figures one can see, the gas temperature in the hearth 5 stays below the setpoint and all temperature measurements in the hearth 4 are also below setpoint, while the gas flows to each burner are permanently at the high limit. Compared to the case presented, most of the time when the furnace operates at the same feed rate the gas flow to the hearth 4 stays lower, while the temperature measured in the hearths 4 and 5 is noticeably higher. Thus, the data presented in Figures 27 and 28 probably represents the conditions in the hearth 4 when the exothermic reaction is not occurring (and therefore not releasing energy) and/or the metakaolin formation consumes more heat than usually, leading to lower temperatures in the hearths.

Furthermore, several instances are observed in the data when the gas flow to one of the burners fluctuates heavily together with the three temperature measurements in the hearth 4, while one temperature measurement in the hearth 4 and the temperature measurement in the hearth 5 are quite stable and follows the setpoint. The ‘switching’ behavior in the hearth 4, as shown in Figure 29, could appear when a big change in the gas flow almost has no effect on the respective temperature measurement. The switching behavior occurs due to the non-linear effect of the gas flow on the temperature. In addition, the fluctuation in the gas flow, as in Figure 30, to maintain the temperature in hearths 4 and 5 might be due to the activation

and deactivation of the exothermic reaction in heath 4. The amount of gas required to maintain the temperature in hearth 4 decreases once the exothermic reaction takes place, and the temperature increases once the exothermic reaction stops occurring.

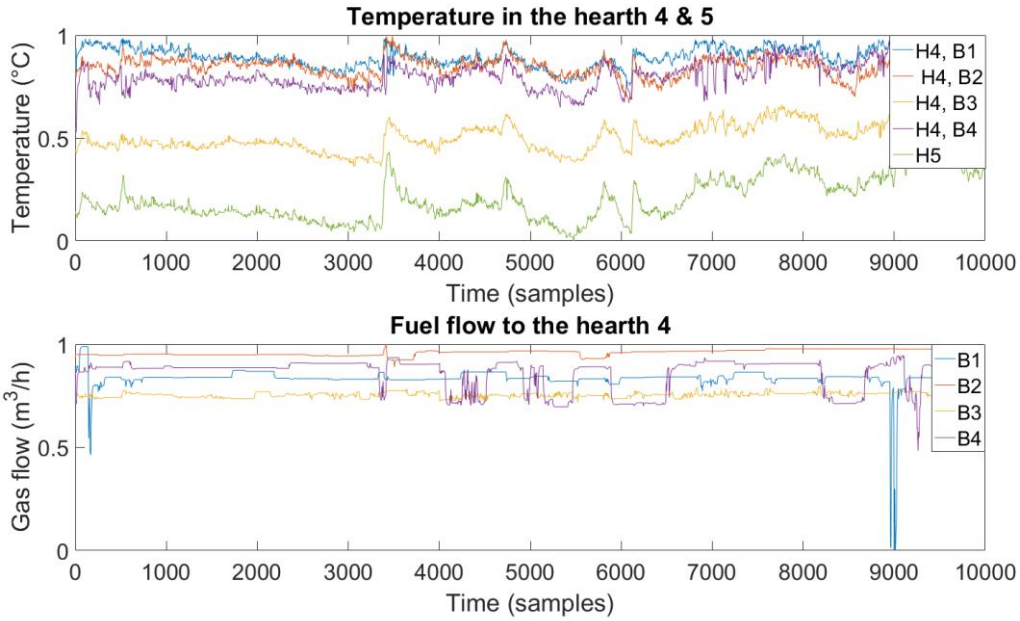


Figure 27: An example when the exothermic reaction does not occur in the hearth 4

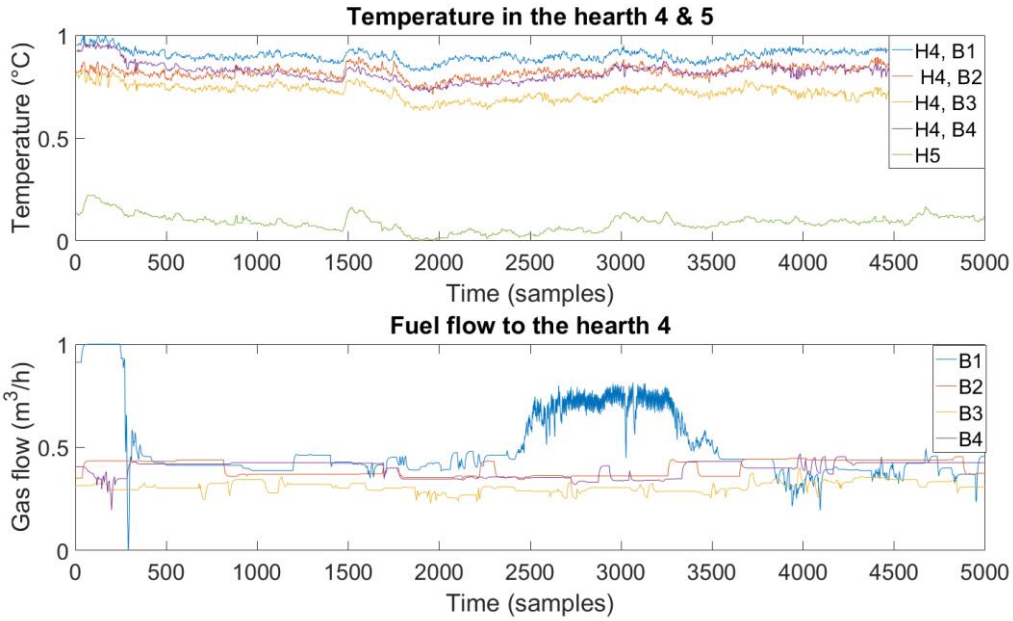


Figure 28: An example when the exothermic reaction does not occur in the hearth 4

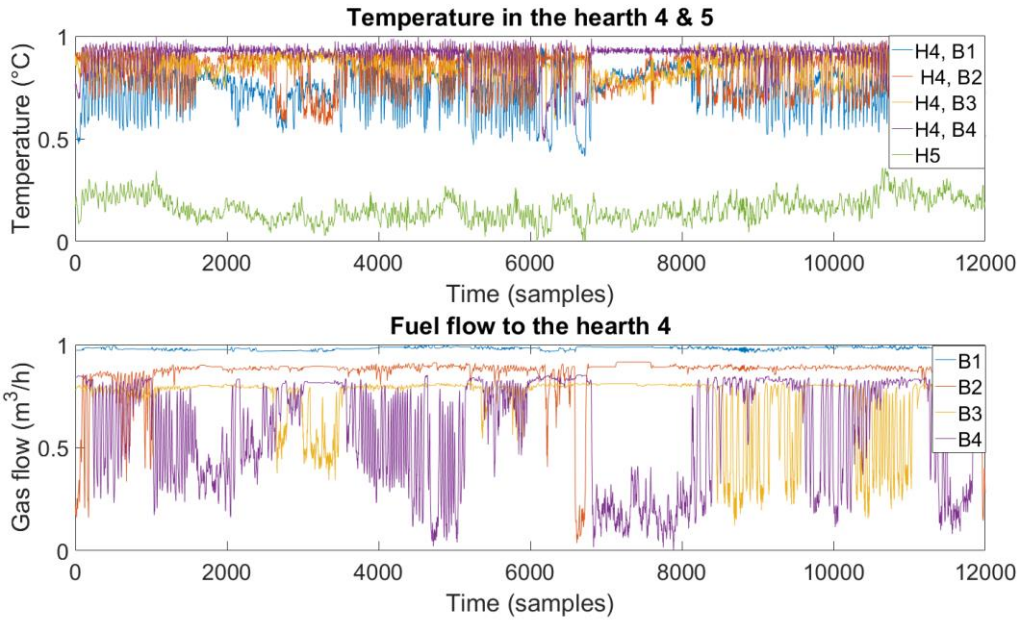


Figure 29: An example of the 'switching' behavior in the hearth 4

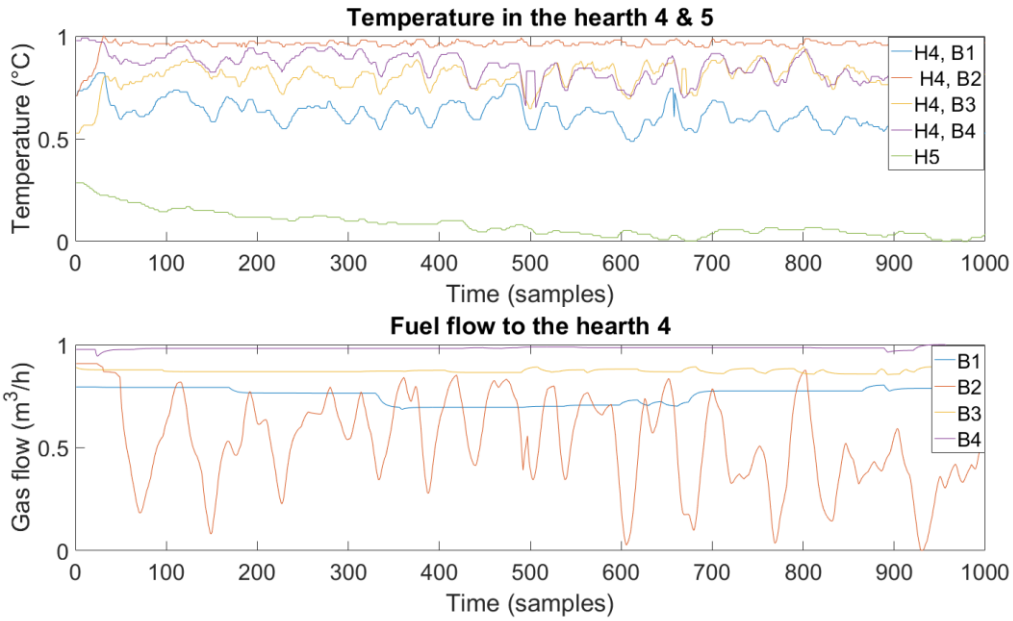


Figure 30: An example when the exothermic reaction activates/deactivates in the hearth 4

The effect of the exothermic reaction rate on the temperature profile in the furnace is also discussed in the case study presented in Gómez Fuentes (2016). To summarize, the increased reaction rate can be recognized when the gas flow to the hearth 4 drops while the gas temperature in the hearth 5 rises. The exothermic reaction and its effect on the process is further analyzed by considering the lower section of the furnace, which is briefly discussed in the next section.

## 7.2 Analysis of the hearths 5- 8

The temperature profile of the hearths 5 - 8 was analyzed starting from the behavior of the temperature measurements in the hearth 8. An interesting observation was found concerning the difference between the two temperature measurements located in different quarters of the hearth 8. In general, it was expected that two temperature measurements in the hearth 8 are close to each other, and therefore there is difference between them stays around zero. However, the actual distribution of the temperature difference is presented in Figure 31 for different feed rates, and two clusters are clearly seen located around 40 °C (cluster 1) and 10 °C (cluster 2). Thus, it can be concluded that the lower section of the furnace sometime behaves non-symmetrically. In other words, there is a difference between the conditions in different quarters of the same hearth. The asymmetric process conditions could have occurred due to the occurrence of exothermic reaction differently in different sections of the hearth 6 and in hearth 4 as discussed in the preceding Section 7.1. For example, in one-quarter the exothermic reaction could start one volume earlier compared to the opposite quarter, leading to a difference between the opposite quarters in the solid and gas temperature through the downstream hearths. However, there are not sufficient process measurements available to determine the reason for the asymmetric behavior seen in the lower section of the furnace.

As the observed temperature difference between the measurements located in the hearth 8 can be related to the exothermic reaction ongoing in the preceding hearths, it is noteworthy to evaluate its effect on the fuel consumption. Since, the asymmetric behavior is observed only on the lower feed rates, the mean fuel consumption of the furnace during the same time period, the time period when temperature measurements were taken, was studied for lower feed rates. Figure 32 illustrates a comparison for the total fuel consumption in the furnace, between active exothermic reaction in the hearth 4 and during the normal operation. The consumption of total gas flow is low when the reaction is active earlier in the hearth 4. This is supported by the tight temperature control; for the event where the reaction occurs actively in the hearth 4, the temperature is self-maintained by the energy released exothermically, causing a decrease of the overall consumption of fuel. The decrease in energy consumption can be strategically used to lower furthermore the fuel consumed in the furnace, with the implementation of the feedforward control.

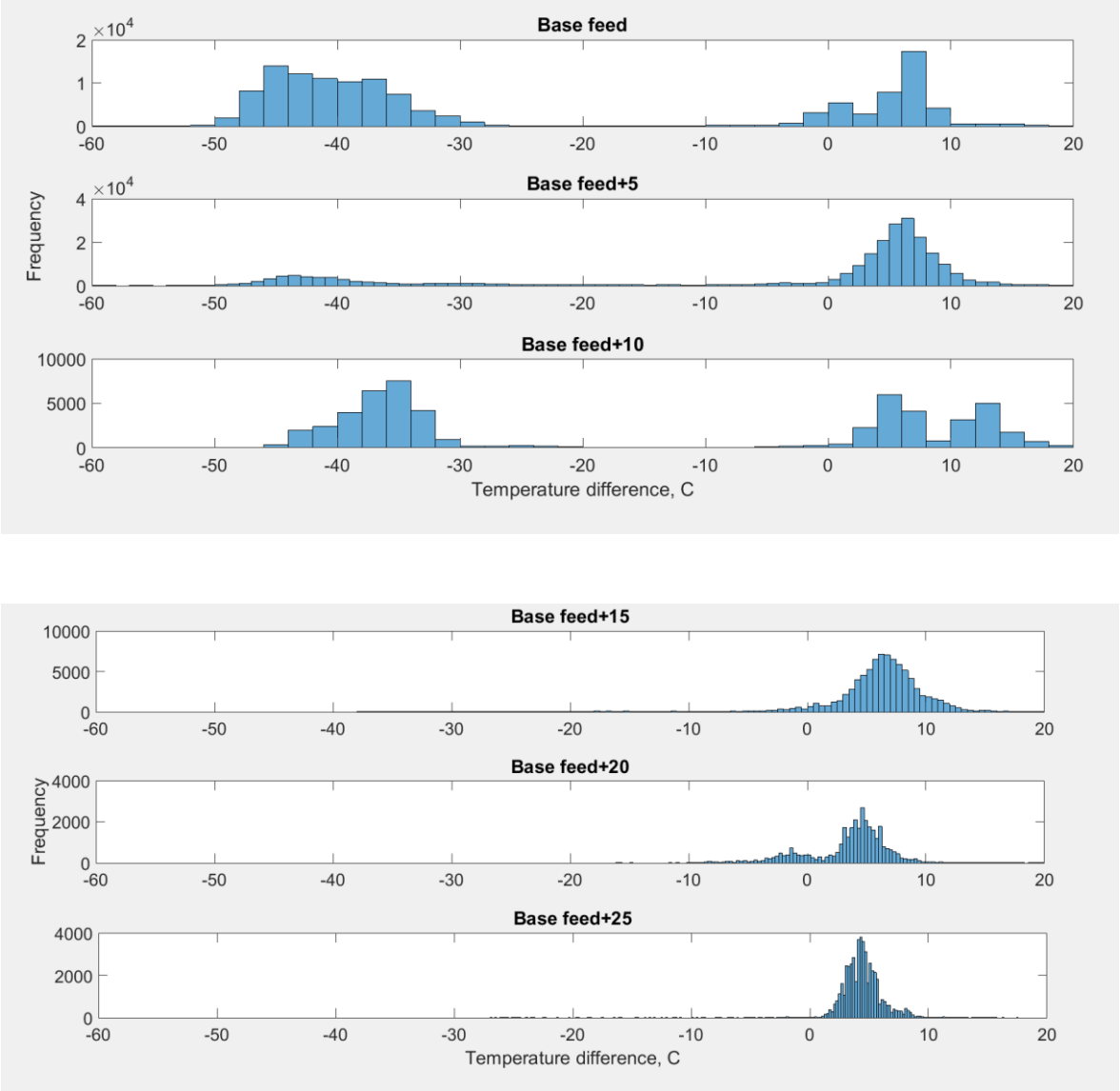


Figure 31: Histogram of the difference between the temperature measurements located in the hearth 8 (top plot for low feed rates, bottom plot for high feed rates)

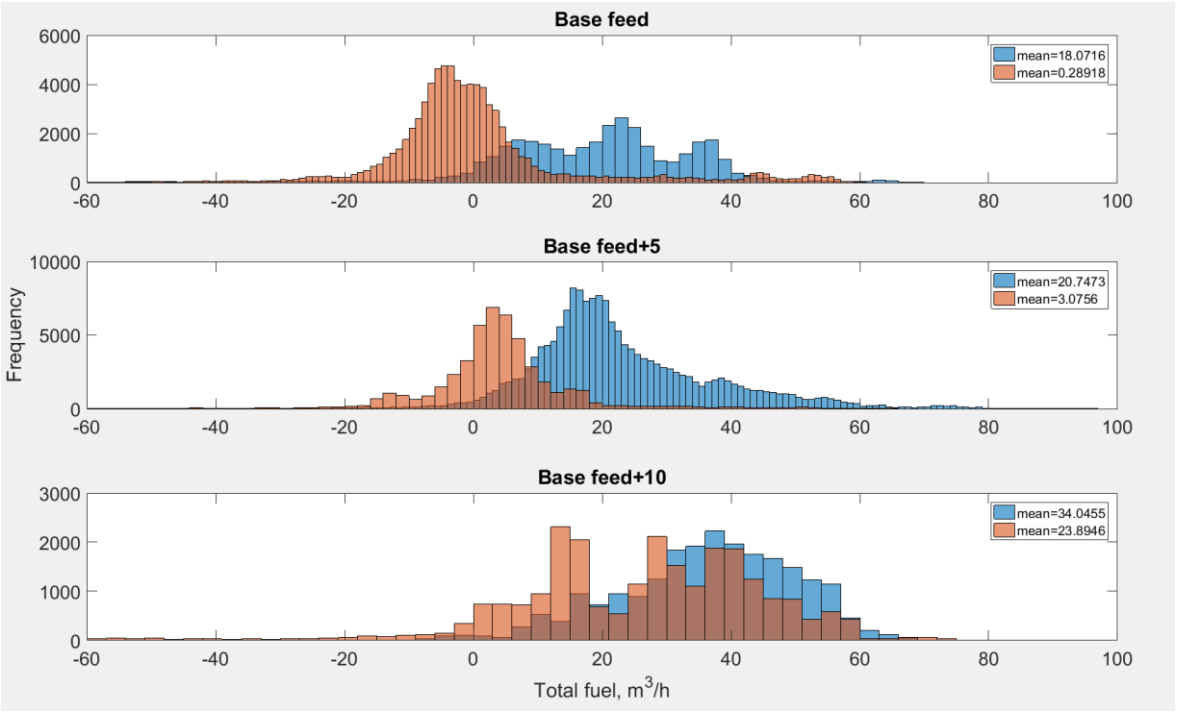


Figure 32: Total gas flow consumption for the active exothermic reaction (orange), and normal operation (light blue)

To conclude, it seems that implementation of feedforward control to optimize the fuel consumption in the hearth 6 based on the energy consumption in the heath 4 (considering the occurrence/non-occurrence of the exothermic reaction) could help in achieving a noticeable reduction in the fuel consumption. However, the benefits on the proposed control strategy cannot be assured for the higher furnace loads. Moreover, further research is needed to evaluate how the variation in normal operation affects the product quality (brightness, soluble aluminum contents) and to determine the favorable operating conditions in the lower section of the furnace to optimize the total gas flow, while stabilizing the temperature in the furnace.

Based on the case study provided in Gómez Fuentes (2016) and the operating mode presented at the beginning of section 7.2, it is clear that presence/absence of the exothermic reaction in the hearth 4 affects the temperature profile of the furnace and its effect is visible in the hearths 4 and 5.

# 8. Control strategies for the temperature profile in the MHF

This section describes the control strategy scheme for the MHF. The main objective of the control strategy is to achieve uniform product quality and optimizing the plant capacity. The overall process control strategy comprises of three different levels: optimizing level, stabilizing level, and the basic level, as shown in Figure 33 below.

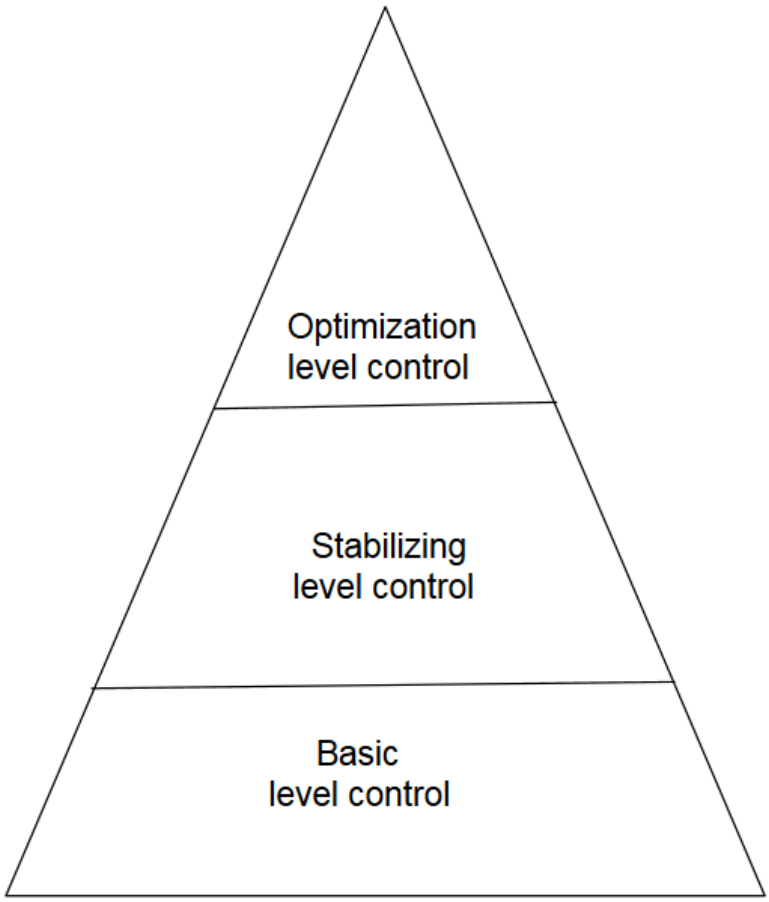


Figure 33: The overall control strategy of the furnace

The optimizing level control aims to select the best operating conditions improving the production capacity, the energy efficiency and achieving the required product quality. The stabilizing level control aims to attenuate the variation in the calcination reactions taking place in the solid phase of the furnace. Basic level controllers are used for control of the

temperatures in the hearths 4 and 6 (hearths, where the burners are placed) with the use of the classical PI controllers.

Data analysis of the furnace, conducted in the previous section, indicated the activation/deactivation of the exothermic reaction in the hearth 4. As a result, variation in temperature profile of the furnace can be clearly seen. In addition, in Gomez Fuentes (2016), the occurrence of the exothermic reaction on the top of the solid layer in the hearth 4 has been discussed. The observed variation (activation/deactivation of the exothermic reaction) clearly affects the operating conditions throughout the furnace, thereby increasing variations in the properties of a final product.

Since, activation/ deactivation of the exothermic reaction was clearly seen in the process, energy balance plays a key role when developing the control strategy for the MHF. Thus, this thesis focus on the development of soft sensor based on the energy balance, which will be later included in the control hierarchy of the furnace. The detail description of the energy balance is explained below.

## 8.1 Soft sensor development based on energy balance calculation

As mentioned in the earlier sections, calcination of kaolin in the MHF is a temperature dependent process and control of the temperature profile to desired value ensures the quality product with constant calcination process. The high temperature in the furnace for heating the solid is obtained from the combustion of methane gas supplied in the hearths 4 and 6. Hence, the solid temperature in the furnace is controlled by controlling the gas flow. It has been mentioned earlier, the temperature in the hearth 6 is critical in determining the quality of the product and hence manipulation of it to the desired value is crucial. Moreover, since, the temperature in hearth 6 is correlated with the reaction occurring in the preceding hearths as well as their temperature, adjusting the temperature in the hearth 6 based on the variation in the temperature in the preceding hearths due to the shifting of reactions as well as other disturbances is fundamental. Identifying the disturbances in the hearths 4 and 5 enables to adjust the temperature in the hearth 6 to ensure the quality of the product and also to optimize the gas flow in the hearth 6. However, it is impractical to investigate when the reactions of kaolin into spinel phase occurs, since there are insufficient measurements available. The soft sensor can be considered as an alternative practical approach in solving this problem. The

soft sensor model based on the energy balance can be developed to estimate the rate of the exothermic reaction of solid occurring in the hearth 4.

Soft sensors are the mathematical models that utilize the relevant variables to estimate the desired unmeasured variable. Soft sensors are considered as a reliable software technique (program) for the estimation of important variables and are often called observers. (Jordaan, et al., 2004) This chapter describes the development of the soft sensor based on the energy balance calculations of the first half of the MHF (hearths 1 to 4) to estimate the rate of the exothermic reaction in the hearth 4. Both steady state (static) and dynamic energy balance models for hearths 1 to 4 were developed to estimate the exothermic reaction rate. Initially, the inflow and outflow of the energy in the system will be discussed followed by the energy balance calculations and the estimation of the ERR.

### 8.1.1 Steady-state energy balance

Energy balances based on the input and output flows were calculated based on the law of energy conservation (Barrie & Mullinger, 2013). The input energy streams are the combustion energy obtained from the hearth 4 by the combustion of methane and combust gas flow from the hearth 5. The amount of air required for the complete combustion of methane was calculated based on the stoichiometric ratio of gas and air. Accordingly, the outflow energy streams are the exhaust gases, solids, and heat losses to the cooling air and the surroundings. Figure 34 shows the energy flow in the first half hearths of the MHF.

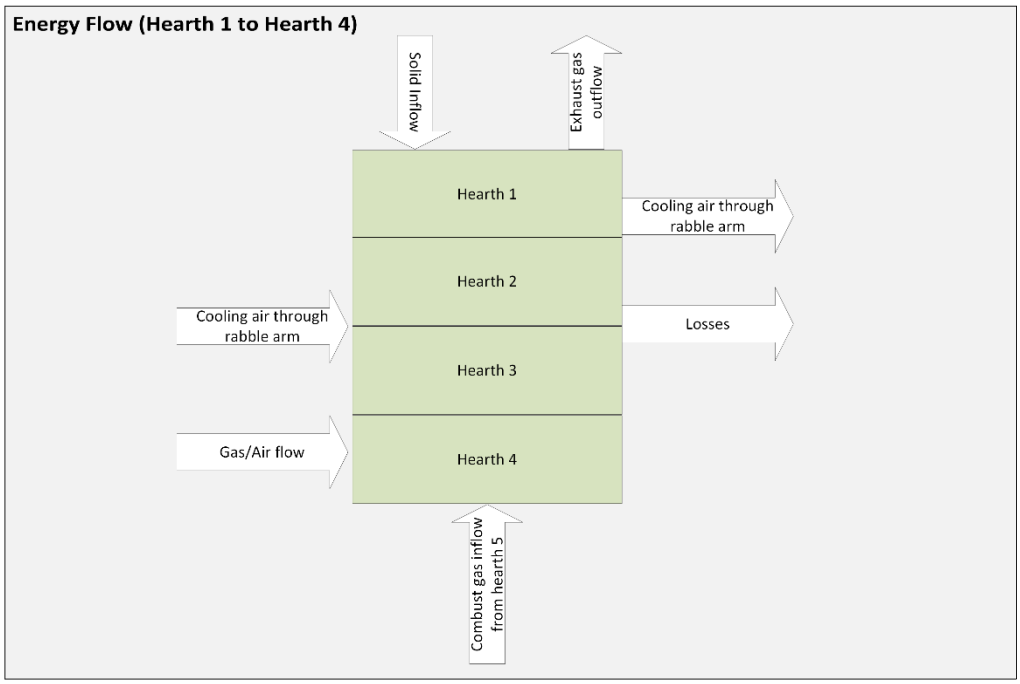


Figure 34: Incoming and outgoing energy flow in the first half section of the multiple hearth furnace

The major heat exchange occurs between the feed and combust gas flowing in reverse directions. The energy balance equation is mathematically divided into two sections: solid phase and gas phase. The general energy balances for the solid phase and gas phase are shown below in Equations 28 and 29.

$$\frac{\partial Q}{\partial t} = \dot{Q}_{s,in} - \dot{Q}_{s,out} - \dot{Q}_{evap} - \dot{Q}_{dehyd} + \dot{Q}_{spin} + Q_{sg} \tag{28}$$

where $\frac{\partial Q}{\partial t}$ is the rate of change of energy with respect to time (assumed to be zero), $\dot{Q}_{\mathrm{s,in}}$ and $\dot{Q}_{\mathrm{s,out}}$ are the enthalpies of the incoming and outgoing kaolin, $\dot{Q}_{\mathrm{evap}}$ is the energy of water evaporated from the solid, $\dot{Q}_{\mathrm{dehyd}}$ is the energy consumed by the dehydroxylation reaction, $\dot{Q}_{\mathrm{spin}}$ is the energy released by the spinel phase formation reaction occurring in the hearth 4, and $Q_{sg}$ is the energy transfer between the solid and the gas phase.

$$\dot{Q}_{g,in} - \dot{Q}_{g,out} + Q_{comb} - Q_{gs} = 0 \tag{29}$$

where $\dot{Q}_{\mathrm{g,in}}$ and $\dot{Q}_{\mathrm{g,out}}$ are the enthalpies of the inflowing and outflowing gases, $Q_{comb}$ is the energy produced by combustion of methane from the burners in the hearth 4, $Q_{gs}$ is the energy transferred between the solid and the gas phase.

The steady-state energy balance, also called static energy balance was calculated using general energy balance equations (28-29). The general energy balance equation can be re-written as follows if the MHF system is considered to be in steady state:

$$\dot{Q}_{s,in} - \dot{Q}_{s,out} - \dot{Q}_{evap} - \dot{Q}_{dehyd} + \dot{Q}_{spin} + Q_{sg} = 0 \quad (30)$$

$$Q_{gs} = \dot{Q}_{g,in} - \dot{Q}_{g,out} + Q_{comb} \quad (31)$$

Substituting $Q_{gs}$ from (31) to (30) and expressing $\dot{Q}_{\text{spin}}$ gives us the following:

$$\dot{Q}_{spin} = -\dot{Q}_{s,in} + \dot{Q}_{s,out} + \dot{Q}_{evap} + \dot{Q}_{dehyd} - (\dot{Q}_{g,in} - \dot{Q}_{g,out} + Q_{comb}) \quad (32)$$

Thus, the exothermic rate of reaction is estimated as the percentage of kaolin transformed to the spinel phase in the hearth 4:

$$ERR(t) = \frac{\dot{Q}_{spin}(t)}{H_3 F(t)}, \quad (33)$$

where $H_3$ is the product formation reaction heat and $F(t)$ is the current feed rate.

The energy flows involved in the right part in (32) are briefly specified below. Initially, few assumptions were considered, which are listed below.

- The heat loss to the surrounding was calculated on Eskelinen (2014) and therefore, the total heat loss to the surround in the first four hearths of the furnace was considered half of the total heat loss in the furnace.
- The estimated solid temperature exiting each hearth were obtained from Eskelinen (2014).
- The exothermic reaction was assumed to begin at the hearth 4.
- The temperature of air cooling the rabble arms was assumed to be about 80 ℃ when entering the hearth 4.

In addition, the standard values of the physical quantities are provided in Table 3 below.

Table 3: Physical quantities and their standard value

| Physical quantities | Value (unit) | Reference |
|---|---|---|
| Heat capacity of water | 4.2 (J/(g*K)) | (Ramsden, 1996) |
| Heat capacity of kaolin | 1.16 (J/(g*K)) | (Schieltz & Soliman, 1966) |
| Heat capacity of metakaolin | 1.19 (J/(g*K)) | (Schieltz & Soliman, 1966) |
| Latent heat of vaporization of water | 2260 (J/(g*K)) | (Ramsden, 1996) |
| Molecular weight of kaolin | 258(g/mol) | (National Center for Biotechnology Information, 2016) |
| Heat for dehydroxylation | 891000(J/kg) | (Eskelinen, et al., 2015) |
| Heat released during spinel phase formation | -2130000(J/kg) | (Eskelinen, et al., 2015) |
| Heat of combustion of Methane | 802000 (J/mol) | (Blok, 2007) |

The initial temperature of the solid was measured to be $T_0$ =30 ℃. The kaolin is dehydroxylated at around $T_{dehyd}$ =450 ℃ and is converted into metakaolin. The energy required for heating and evaporating the free water is:

$$\dot{Q}_{evap} = 0.005\, F\big(C_{p,w}(100 - T_0) + H_{evap}\big), \tag{34}$$

where $F$ is the feed rate of the solids, $C_{p,w}$ is the heat capacity of water, and $H_{evap}$ is the heat of water vaporization.

The energy of the dehydroxylation is:

$$\dot{Q}_{dehyd} = (1 - 0.005)F * H_{dehyd}, \tag{35}$$

where $H_{dehyd}$ is the heat of dehydroxylation reaction.

The energy of the inflow is calculated as:

$$Q_{s,in} = \big(0.995C_{p,k} + 0.005C_{p,w}\big)FT_0, \tag{36}$$

where $C_{p,w}$ and $C_{p,k}$ are the heat capacity of water and kaolin respectively.

The energy of the solids leaving the furnace is calculated as:

$$Q_{s,out} = 0.995F(C_{p,k}\big(T_{dehyd} - T_0\big) + 0.86C_{p,m}(T_5 - T_{dehyd}), \tag{37}$$

where $C_{p,m}$ is the heat capacity of the metakaolion and $T_5$ is the temperature measurement at the beginning of the hearth 5.

Methane is the source of energy for kaolin calcination. Combustion of methane in the presence of oxygen releases the great amount of energy, calculated as follows:

$$Q_{comb} = V_{meth} * H_{comb}, \quad (38)$$

where $V_{meth}$ is the flow of methane to the hearth 4, and $H_{comb}$ is the combustion heat. The energy of the gases entering the hearth 4 from the hearth 5 is computed according to:

$$\dot{Q}_{g,in} = \dot{Q}_{O_2,in} + \dot{Q}_{N_2,in} + \dot{Q}_{H_2O,in} + \dot{Q}_{CO_2,in}, \quad (39)$$

where the enthalpy of the components $\dot{Q}_{O_2,in}$, $\dot{Q}_{N_2,in}$, $\dot{Q}_{H_2O,in}$ and $\dot{Q}_{CO_2,in}$ is calculated according to the method used in Eskelinen et. al. (2014). Similarly, the enthalpy of the gas outflow $\dot{Q}_{g,out}$ is calculated.

### 8.1.2 Dynamic energy balance

Along with the steady-state energy balance, the dynamic energy balance was calculated considering the variations in the feed rate along with the time. In particular, the energy consumed by solids in each hearth is calculated separately based on the amount of solid in the hearth. The temperature of solid estimated for each hearth and the residence time distribution in each hearth are listed in Table 4 below (Eskelinen, 2014).

Table 4: Estimated temperature of solid and residence time distribution in each hearth

| Hearth | Estimated solid Temperature (°C) | Residence time distribution (seconds) |
|---|---|---|
| 1 | 70 | 156 |
| 2 | 119 | 124 |
| 3 | 475 | 534 |
| 4 | 565 | 276 |

The amount of feed to each hearth was calculated based on the feed rate and the residence time distribution between the hearths, as listed in Table 4:

$$M_i = \int_{t(i)}^{t(i+1)} F(t)dt, \quad (40)$$

where $i$ is a hearth number, and $t(i)$ is the total time (in seconds) spent by the solids in the first $i-1$ hearths. Next, it is assumed that 20% of kaolin is converted into metakaolin in the

hearth 3 and the rest of the transformation occurs at the hearth 4. The energy consumed in the hearth is then calculated as follows:

$$Q_{h1} = 0.995 M_1 C_{p,k} * (T_1 - T_0) \quad (41)$$

$$Q_{h2} = 0.005 M_1 (C_{p,w}(100 - T_0) + H_{evap} + 0.995 M_1 C_{p,k} * (T_2 - T_1) \quad (42)$$

$$Q_{h3} = 0.995 M_1 C_{p,k} * (T_{dehyd} - T_2) + 0.2 * 0.995 M_1 * H_{dehyd} + 0.2 * (0.995 - 0.14) M_1 C_{p,mk} * (T_3 - T_{dehyd}) + 0.8 * 0.995 M_1 C_{p,k} * (T_3 - T_{dehyd}) \quad (43)$$

$$Q_{h4} = 0.2 * (0.9950.14) M_1 * C_{p,mk}(T_{dehyd} - T_3) + 0.8 * 0.995 M_1 C_{p,k} * (T_{dehyd} - T_3) + 0.8 * \frac{0.995 M_1}{MW_k} * H_{dehyd} + (0.995 - 0.14) M_1 C_{p,mk}(T_4 - T_{dehyd}), \quad (44)$$

where $M_1$ is the mass of the feed, $C_{p.w}, C_{p,k}$, and $C_{p,mk}$ are the heat capacity of water, kaolin, and metakaolin respectively, $T_i$ is the temperature of feed exiting the $i_{th}$ hearth ($i$ = 0, is the feed temperature in the initial stage).

The gas phase of the dynamic energy balance is similar to the static as the dynamics of the gas phase are much faster than the solid phase.

## 8.2 Comparison of static and dynamic energy balance

The steady-state energy balance and dynamic energy balance resembles each other on the constant feed rate. During the step change of the feed rate, as presented in Figure 35(b), the gas consumption in the hearths 4 and 6 is changing slowly, with the complete transition taking about 42 minutes. Indeed, the fuel consumption is adjusted according to the amount of solid in the hearths, which is changing slowly after a feed rate step due to solids transport phenomena. Thus, the transition time in the fuel consumption agrees with the known residence time of the solids in the furnace, which is about 42 minutes. The static soft-sensor, calculating the amount of solids in the hearths according to the current feed rate, is, therefore, unable to correctly consider the solids transport phenomena in the furnace. In the results, the unrealistic peaks in the exothermic reaction rate estimation are produced by the static soft sensor, as demonstrated in Figure 35(a). Actually, the static soft-sensor estimation of the

energy consumption by the solids has ultimately changed simultaneously with the step of the feed rate, which resulted in overestimating the energy released by the exothermic reaction. However, in the soft-sensor utilizing the dynamic energy balance, the effect of the feed rate change on the energy consumption by the solid phase is estimated taking into account the transportation delays within the furnace. This allows to produce an adequate estimation of the exothermic reaction rate in the hearth 4, as confirmed by figures below.

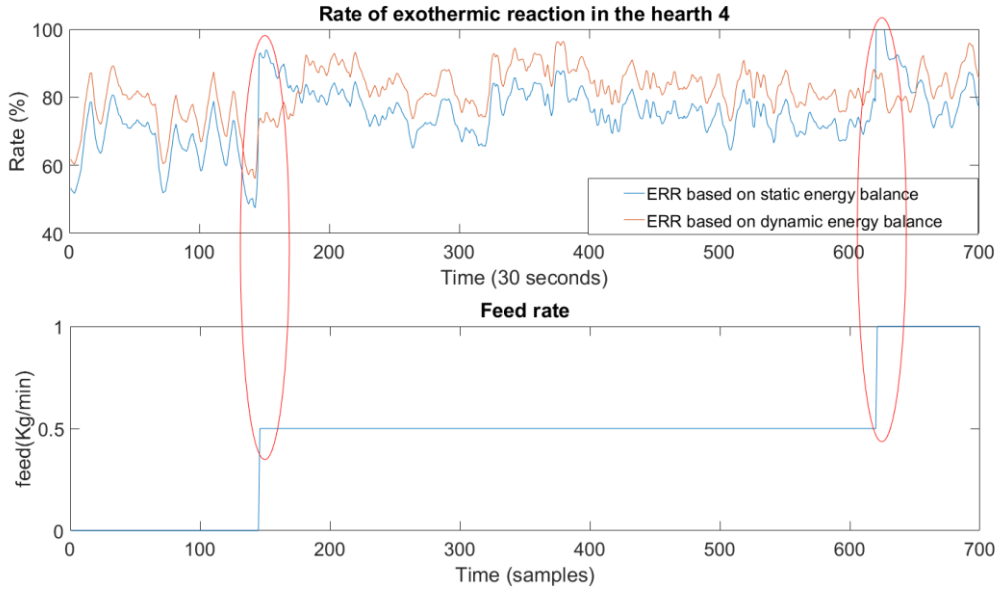


Figure 35: The results of the dynamic (in blue) and static (in red) soft sensors to estimate the rate of exothermic reaction in the hearth 4 (top) along with the feed rate step change (bottom)

# 9. Conclusions

In this thesis, a review of the control strategies used in furnace's temperature profile control is provided. In fact, most of the literature is focused on the gas temperature control, which helps to attenuate variations in the solid temperature profile but cannot remove the variations completely because of the varying ore properties. Moreover, in the considered furnace there are not enough actuators (burners) to control the gas temperature profile, which makes most of the control methods found in the literature inapplicable.

In the experimental part of the thesis, the major disturbance affecting the whole temperature profile in the furnace was discovered by a databased analysis, and the related process phenomena were discussed. The different conditions observed in the hearth 4, activation and deactivation of the exothermic reaction during the process, show the variation in the temperature profile of the furnace.

Hence, this thesis was focused on the development of energy balance based soft sensor to estimate the intensity of the exothermic reaction. The soft-sensor to estimate the exothermic reaction in the hearth 4 was developed using the energy balance of first four hearths. The comparison of the static and the dynamic soft-sensors was also carried out and it demonstrated that the dynamic method is more accurate because it properly takes into account the residence time of the solids in the MHF. The developed soft sensor will be later implemented in the overall control strategy of the furnace.

# References


Akalp, M., Dominguez, A. & Longchamp, R., 1994. Supervisory fuzzy control of a rotary cement kiln. *Proceedings of the Electrotechnical Conference, 1994,* Volume 2, pp. 754-757.

Barrie, J. & Mullinger, P., 2013. An Introduction to Heat Transfer in Furnaces. In: *Industrial and Process Furnaces.* Oxford: Elsevier Ltd., pp. 98-138.

Blok, K., 2007. Higher and lower heating value of fuels. In: *Introduction to Energy Analysis.* Amsterdam: Techne Press, p. 29.

Chandrasekhar , S., Ramaswamy & Ramaswamy , S., 2002. Influence of mineral impurities on the properties of kaolin and its thermally treated products. *Applied Clay Science,* 21(3-4), pp. 133-142.

Doane, . E. P., 1968. *Temperature control in multi-zone heat exchange operation.* United States of America, Patent No. US3406740 A.

Eskelinen, A., 2014. *Dynamic modelling of a multiple hearth furnace ,* Espoo, Finland: Aalto University.

Eskelinen, A., Zakharov, A., Jämsä-Jounela, S.-L. & Hearle, J., 2015. Dynamic Modeling of a Multiple Hearth Furnace for Kaolin Calcination. *AIChE Journal,* 61(11), p. 3683–3698.

Galvez, J. & de Araujo, L., 1996. A multivariable PI controller for nonlinear ill-conditioned electrical tubular ovens. *Circuits and Systems,* Volume 3, pp. 1005 - 1008.

Ghosh, A. & Ray, H. S., 2001. Methods of extraction and refining of metals. In: *Principles of Extractive metallurgy.* New Delhi: New Age Internation (P) Ltd., publishers, p. 15.

Gómez Fuentes, J. V., 2016. *Simulation Environment for Advanced Control Development of a Multiple Hearth Furnace,* Espoo: Aalto University.

Hennion, F. J., 1986. *The Reclamation of Spent Hydrogenation Catalysts.* Champaign, American Oil Chemists' Society, pp. 172-183.

Insley, H. & Ewell, R. H., 1935. Thermal behavior of the kaolin minerals. *Journal of Research of the National Bureau of Standards,* 14(5), pp. 615-627.

Jordaan, E., Kordon, A., Chiang, L. & Smits, G., 2004. Robust Inferential Sensors Based on Ensemble of Predictors Generated by Genetic Programming. In: *Parallel Problem Solving from Nature - PPSN VIII.* Heidelberg: Springer Berlin Heidelberg, pp. 522-531.

LL Kilns, 2010. *Spec-Zone-Control.* [Online]
Available at: http://www.brackers.com/wp-content/uploads/2015/02/Spec-Zone-Control.pdf
[Accessed 27 04 2016].

McIntyre, G. C., Lacombe, R. J. & Forbess, R. G., 1991. *Furnace combustion zone temperature control method.* United States of America, Patent No. 5,018,458.

Mcketta, J. J. & Cunningham, W. A., 1978. Calcination Equipment. In: *Encyclopedia of Chemical Processing and Design: Volume 6-Calcination Equipment to Catalysis.* New York: Marcel Dekker, Inc., pp. 11-13.

Moon, U.-C. & Lee, K. Y., 2000. Temperature Control of Glass Melting Furnace With Fuzzy Logic and Conventional PI Control. *American Control Conference, 2000. Proceedings of the 2000 , IEEE,* Volume 4, pp. 2720 - 2724.

Murray, H. H., 2006. Exploration, Mining, and Processing. In: *Applied Clay Mineralogy: Occurrences, Processing and Applications of Kaolins, Bentonites, Palygorskitesepiolite, and Common Clays.* Indiana: Elsevier Science, pp. 74-75.

Mzyk, G., 2014. Hammerstein System. In: *Combined Parametric-Nonparametric Identification of Block-Oriented Systems.* s.l.:Springer International Publishing, pp. 23-85.

National Center for Biotechnology Information, 2016. *PubChem Compound Database; CID=56841936.* [Online]
Available at: https://pubchem.ncbi.nlm.nih.gov/compound/56841936
[Accessed 11 06 2016].

Ogunnaike, B. A. & Ray, W. H., 1994. Design of Multivariable controllers. In: *Process Dynamics, Modeling, and Control.* New York: oxford University Press, pp. 776-777.

Pruett, R. J. & Pickering, S. M. J., 2006. Kaolin. In: J. E. Kogel, C. N. Trivedi, J. M. Barker & S. T. Krukowski, eds. *Industrial Minerals and Rocks:Commodities, Markets, and Uses.* Littleton: Society for Mining, Metallurgy, and Exploration, Inc. (SME), pp. 383,394.

Ptáček, P. et al., 2010. The kinetics of Al–Si spinel phase crystallization from calcined kaolin. *Journal of Solid State Chemistry,* 183(11), pp. 2565-2569.

Ramsden, E., 1996. The hydrosphere. In: *Chemistry of the Environment.* Cheltenham: Stanley Thornes Publishers, Ltd, p. 69.

Rasmussen, K. E. et al., 2015. Comparison of the Pozzolanic Reactivity for Flash and Soak Calcined Clays in Portland Cement Blends. In: K. Scrivener & A. Favier, eds. *Calcined Clays for Sustainable Concrete : Proceedings of the 1st International Conference on Calcined Clays for Sustainable Concrete.* Zürich: Springer, pp. 151-157.

Salvador, S., 1995. Pozzolanic properties of flash-calcined kaolinite: a comparative study with soak-calcined products. *Cement and concrete research ,* 25(1), pp. 102-112.

Sauermann , H., Stenzel, . C., Keesmann, S. & Bonduelle, B., 2001. High-Stability Control of Multizone Furnaces using Optical Fibre Thermometers. *Crystal Research and Technology,* 36(12), pp. 1329-1343.

Schieltz, N. & Soliman, M., 1966. *Thermodynamics of the various high temperature transformations of Kaolinite.* NewYork, Pergamon Press, pp. 419-428.

Sell, N. J., 1992. Methods for water pollution control. In: *Industrial Pollution Control: Issues and Techniques.* New York: JOHN WILEY & SONS, INC., p. 84.

Smith, R., 2005. Heat Exchanger Networks I- Heat Transfer Equipment. In: *Chemical process: design and integration.* Chichester: John Wiley & Sons, p. 348.

Stadler , K. S., Poland, J. & Gallestey, E., 2011. Model predictive control of a rotary cement kiln. *Control Engineering Practice,* 19(1), pp. 1-9.

The Great Soviet Encyclopedia, 1970-1979. *Kaolinization.* [Online]
Available at: http://encyclopedia2.thefreedictionary.com/Kaolinization
[Accessed 18 06 2016].

Thomas, R. E., 2010. *High Temperature Processing of Kaolinitic Materials,* Birmingham: eTheses Repository, The University of Birmingham.

Thurlow, C., 2005. *China clay from Cornwall & Devon, An illustrated account of the modern China Clay Industry.* 4th ed. St Austell: Cornish Hillside Publications.

Valiquette, J., Savoie, M. & Leclerc, M., 1997. *Practical aspects of model predictive control implementation on an industrial lime kiln.* Brussels, IEEE Conference Publications, pp. 2711 - 2715.

Zhou, X., Yu, S., Yu, J. & Liang, . L., 2004. Multivariable temperature measurement and control system of large-scaled vertical quench furnace based on temperature field. *Journal of Control Theory and Applications,* 2(4), pp. 401-405.